Water-Soluble Noble Metal Nanoparticle Catalysts Capped with Small Organic Molecules for Organic Transformations in Water

*Al-Mahmnur Alam and Young-Seok Shon**

Department of Chemistry and Biochemistry and the Keck Energy and Materials Program (KEMP), California State University, Long Beach, 1250 Bellflower Blvd., Long Beach, CA 90840, Unites States

KEYWORDS. Nanoparticle, Catalysis, Semi-heterogeneous, Nobel metal, Hydrogenation, Coupling reaction, Green catalysis, Biphasic catalysis.

ABSTRACT. This article recaps a variety of interesting catalytic studies based on solubilized and freely movable noble metal nanoparticle catalysts employed for organic reactions in either pure water or water-organic biphasic systems. Small organic ligands-capped metal nanoparticles are fundamentally attractive materials due to their enormous potential as a well-defined system that can provide spatial control near active catalytic sites. The nanoparticle catalysts are first grouped based on the synthetic methods (direct reduction, phase transfer, and redispersion) and then again based on the type of reactions such as alkene hydrogenation, arene hydrogenation, nitroaromatic reduction, carbon-carbon coupling reactions, etc. The impacts of various ligands

on the catalytic activity and selectivity of semi-heterogeneous nanoparticles in water are discussed in detail. The catalytic systems using polymers, dendrimers, and ionic liquids as supporting or protecting materials are excluded from the subjects of this review.

1. INTRODUCTION

Noble metals such as ruthenium (Ru), rhodium (Rh), palladium (Pd), silver (Ag), iridium (Ir), platinum (Pt), and gold (Au) have gained compelling reputations as chemically dynamic materials.[1-6] Especially, with the possession of highly reactive surfaces arising from the high surface to volume ratio along with a low number of atomic neighbors, noble metal nanoparticles have been regarded as practical candidates for many areas of catalysis.[6-12] The applications of noble metal nanoparticles in catalysis commonly accompany with the use of superficial solid support to circumvent the stability problems.[13-15] In this condition, catalysis reaction is undertaken in a heterogeneous condition while metal nanoparticles are adsorbed on to a surface by either chemical or mechanical forces. The advantages of this heterogeneous set-up besides the improved stability from nanoparticle aggregation or degradation include a facile separation of products from the catalyst and an easy recycling of the catalyst. However, the overall activity and selectivity of metal nanoparticles in this heterogeneous system can be negatively affected due to the lack of diffusion and the involvement of different surface sites in catalytic reactions.

Without a solid support, metal nanoparticle catalysts stabilized by organic ligands including surface-immobilized small ligands, dendrimers, and polymers can be mobilized in liquid phases as semi-heterogeneous catalysts, having the characteristics of homogenously soluble catalysts with heterotopic surfaces.[8-12] Depending on the structure and functionality of

surface-immobilized organic ligands, noble metal and other transition metal nanoparticles can be dissolved or well dispersed in organic or aqueous solvents in a homogeneous-like condition during the catalytic reactions.[16-18] This would promote not only the activity of metal nanoparticle catalysts but also the selectivity by evenly distributing surface chemistry throughout the reaction mixture. The catalytic reactions of metal nanoparticles are not limited to a single site and can be further tuned by controlling the type and density of surface-immobilized ligands.[16-19] For example, alkanethiolate-capped Pd nanoparticles (PdNPs) with varying surface ligand densities are used for selective hydrogenation and/or isomerization of allylic alcohols, propargylic alcohols, and dienes and chemoselective hydrogenation of olefins with other reactive functional groups.[20-26]

One of the current issues associated with catalysis in organic reactions arises from the pollution impact related to the use of toxic organic solvents. Non-flammable and environmentally friendly characteristics of water certainly make it an excellent choice as a solvent for various catalysis applications.[27-30] Especially, the biocatalysis applications of metal nanoparticles in both academic and industrial sectors must rely on the water-based reactions.[31-33] To fully take advantage of water as a solvent for semi-heterogeneous nano-catalytic reactions, it is important to prepare catalytic metal nanoparticles that can be readily dissolved or dispersed in water. This is one of the main reasons why the synthesis of water-soluble and hydrophilic functionalized nanoparticle catalysts has been intensely studied by nanoscience and catalysis research communities.[34-36] For instance, different biological methods have been explored for the synthesis of water-soluble nanoparticle catalysts such as semi-natural cellulose-stabilized Pd nanoparticles for selective hydrogenation of acetylene.[37,38] In addition, a wide range of water-soluble organic stabilizers, such as dendrimers,[39-41] polymers,[41-44] and small binding ligands such

as carboxylates and thiols,[11,12,16,17] have been used for coating the surface of metal nanoparticle catalysts.

This review is partitioned by both the synthetic methods and the type of organic reactions studied for noble metal nanoparticle catalysts dissolved or fully dispersed in water. The first part introduces the representative synthetic methods for various water-soluble noble metal nanoparticle catalysts that are not bound to any solid support such as metal oxide, silica, or polymer particulate based materials. The second part is focusing on the aqueous or biphasic reactions performed with various noble metal nanoparticle catalysts. A variety of catalytic studies in which water-soluble metal nanoparticles with small surface-immobilized ligands (e.g. citrate, thiols, amines, ammonium halides, etc.) and small supramolecules (e.g. α, β, γ-cyclodextrins, etc.) that act as effective stabilizers are introduced. "Ligand-less" metal nanoparticle catalysts are also briefly discussed in this review, but with an alternative interpretation.[45,46] Dendrimers and polymers-stabilized metal nanoparticles[47-51] and solvent (e.g. ionic liquid)-stabilized metal nanoparticle catalytic systems[52] are not covered in this review. Non-organic reactions such as water splitting[53,54] are also not covered in this review. These topics have been extensively covered by other review articles.[47-54]

2. SYNTHESIS OF WATER-SOLUBLE METAL NANOPARTICLES

Many review papers have been published in the subject of metal nanoparticles soluble in aqueous conditions and their potential catalytic applications, but their main focuses were placed on the limited scopes in catalytic materials with specific capping ligands or core metals, and/or in specific reaction types.[55-57] In comparison, this review has a distinctive approach with a focus on

water-soluble noble metal nanoparticles synthesized in solution phase and used for various organic transformation reactions.

Several different strategies have been employed for the synthesis of water-soluble noble metal nanoparticles in liquid phase for catalysis applications: 1) **direct** reduction in water, 2) **phase transfer** from organic to aqueous phases, and 3) **re-dispersion** of nanoparticles in water after reaction solvent removal. The obvious choice and the most popular one is the direct reduction of water-soluble metal complexes by some kinds of reducing agents in neat water. Many occasions the reductants also act as the stabilizing ligands or agents. In other cases, another capping agents or surfactants are used besides the reducing agents to prevent the aggregation of nanoparticles and also to control the size or shape of nanoparticles. The phase transfer methods are employed when the reduction of metal precursors and the passivation of growing nanoparticles initially take place in organic phase. Eventual *in situ* phase transfer from organic phase to aqueous phase involves the immobilization of water-soluble ligands on metal nanoparticle surfaces. When the mixed solvents (e.g. ethanol and water or acetone and water) are used for the reduction of organometallic complexes, these solvent mixtures need to be removed after the completion of nanoparticle formation. Re-dispersion of metal nanoparticles in water is achieved by using water-soluble ligands that can be immobilized on nanoparticle surfaces. These three methods are discussed in depth in the following sub-sections and summarized in Scheme 1.

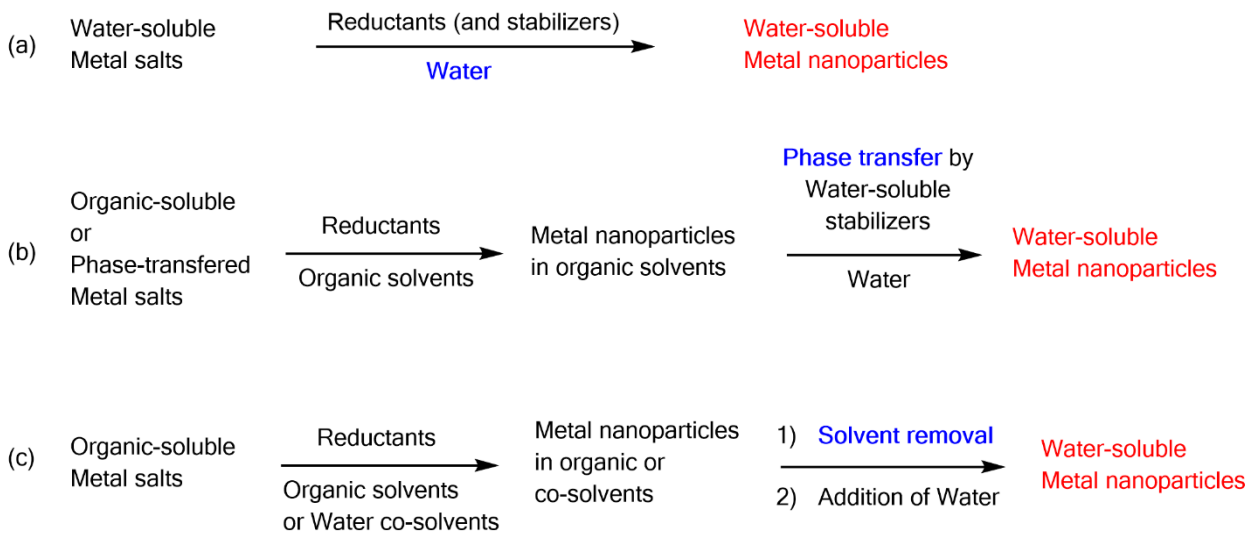

Scheme 1. Three different methods employed for the synthesis of water-soluble noble metal nanoparticles: (a) Direct reduction method, (b) Phase transfer method, and (c) Redispersion method.

2.1. Direct Reduction in Water

Synthesis of noble metal nanoparticles in water has a long history dating back to the preparation of Au and Ag colloidal solutions that are often used for decoration purposes.[58] One of the most popular synthetic methods for metal colloids is the Turkevich method initially reported in 1951[59] and upgraded later by several other research groups.[60-62] Herein, this section focuses on water-soluble noble metal nanoparticles stabilized by various organic ligands (Figure 1) that are synthesized by direct reduction method in neat water and used for the subsequent catalysis of organic molecules (Table 1).

The Turkevich method to synthesize water-soluble metal nanoparticles utilizes trisodium citrate (**1**) as both reducing agent and stabilizer.[59-62] However, the low colloidal stability of citrate-stabilized metal nanoparticles have made this method less efficient in producing

nanoparticle catalysts with a broad range of applications. Limited examples include the uses of citrate-capped Au and Ag nanoparticles (AuNPs and AgNPs) for organic transformations such as the reduction of 4-nitrophenol, Rhodamine B, and benzaldehyde.[63-67] Ag core-Pd shell bimetallic nanoparticles synthesized using this citrate reduction and stabilization protocol have been tested for decomposition of dyes such as Congo red, Direct blue 14, and Sunset yellow.[68] The problem associated with the citrate capping could be somewhat elucidated by introducing additional water-soluble ligands such as thiolated polyethyleneglycol or thiolated poly(acrylic acid) ligands that have stronger interactions with metal surface.[66,67] Although this strategy of replacing citrates with thiols has been proven to be less than fully efficient,[69] the produced water-soluble thiolate-stabilized Au nanoparticles (AuNPs) exhibited good stability and catalytic activity toward the reduction of 4-nitrophenol.[66,67] Citrate ligands on Ag nanoparticles could also be replaced by tannic acid (**2**) and the generated tannic acid-stabilized Ag nanoparticles were more stable and effective for the reduction of Rhodamine B.[63]

Tannic acid (**2**) itself could be used for the reduction of $HAuCl_4$ in water and the subsequently formed tannic acid-stabilized Au nanoparticles showed catalytic activity toward the reduction of 4-nitrophenol.[70] The direct reduction of metal salts by a reagent that can also act as capping ligands have appeared in literatures many times besides the case of tannic acid. Cobaticinium chloride (**3**) has been used for the stabilization of Rh nanoparticles (RhNPs) that were catalytically active for a variety of reactions including ammonia borane hydrolysis, reduction of 4-nitrophenol, transfer hydrogenation, and arene hydrogenation.[71] The active reducing agent for the reduction of $RhCl_3$ was cobaltocene that is derived from cobaticinium chloride. Glucose (**4**) was found to reduce $Pd(acetate)_2$ and protect the resulting Pd nanoparticles in water.[72] These Pd nanoparticles presented a catalytic utility for biphasic homocoupling of aryl

halides. Anionic water-soluble leaning pillar[6]arene (AWLP6, **5**) has been applied for the reduction of $HAuCl_4$ in water.[73] AWLP6 was able to stabilize the produced Au nanoparticles that could catalyze the reduction of 4-nitrophenol. Cyclodextrin (**6a**) was reported to reduce $HAuCl_4$ in basic water with the aid of thermal energy (60 °C).[74] The protection of Au nanoparticles with cyclodextrin allowed the catalytic reaction of these nanoparticles for the reduction of 4-nitrophenol. The alcohol functional groups of hydroxypropyl-α-cyclodextrin (**6b**) could also reduce $PdCl_2$ in water.[75] Cyclodextrin-stabilized Pd nanoparticles produced in this manner was able to catalyze various C-C coupling reactions such as Heck, Suzuki, and Sonogashira reactions.

Only a part of stabilizing ligands acting as a reducing agent for metal salts to form metal nanoparticle catalysts has also appeared in the literatures. When tetrabutylammonium bromide (TBAB, **7**) was introduced to the solution containing $PdCl_2$ in water at high temperature (80 °C – 100 °C), Br^- could operate as a reducing agent while TBAB as a whole could protect the produced Pd nanoparticles.[76,77] The Pd nanoparticles were active for tandem enyne formation via coupling-elimination and tandem Knoevenagel condensation - Michael addition reactions. Similarly, Br^- in TBAB could reduce $PdCl_2$ in water under ultrasonic irradiation.[78] These TBAB-protected Pd nanoparticles were found to catalyze Heck coupling reactions *in situ*.

Reduction of metal salts with reducing agents in the presence of another chemical that functions as a stabilizing ligand is one of the most popular strategies employed in the synthesis of catalytically active metal nanoparticles in water. Among various options of reducing agents, sodium borohydride has been the most popular choice for the reduction of various metal complexes. The relatively slow decomposition rate of $NaBH_4$ especially in basic water directly contributed to the high utility of this reducing agent for various reduction reactions including the reduction of metal ions in aqueous conditions. $NaBH_4$ reduction of $RhCl_3$ and $RuCl_3$ in the

presence of hydroxyl-functionalized tetraalkyl ammonium bromide (or chloride or other anions, **8**) was popularized by Roucoux et al. for the synthesis of water-soluble catalytic Rh and Ru nanoparticles.[79-86] These surfactant-stabilized Ru and Rh nanoparticles exhibited good catalytic activities for the hydrogenation of various aromatic compounds in biphasic conditions. Roucoux et al. and others have also applied the same $NaBH_4$ reduction strategy for the synthesis of Ru and Rh nanoparticles with other stabilizing ligands such as methylated cyclodextrin (**6c**), N-methylephedrium salts (**9**), and polyhydroxylated ammonium chloride (**10**).[87-90] These Ru and Rh nanoparticles have shown activities for the hydrogenation of aromatics, the asymmetric hydrogenation of ethylpyruvate, and the tandem dehalogenation and hydrogenation of halogenoarenes. $Ru(NO)(NO_3)_3$ could also be reduced by $NaBH_4$ in the presence of cyclodextrin (**7**) resulting in the formation of strongly active Ru nanoparticles for the hydrogenation of aromatics, olefins, and carbonyl compounds.[91]

$NaBH_4$ reduction protocol was also utilized for the synthesis of other metal nanoparticles such as Ir and Pd nanoparticles. $IrCl_3$ was reduced by $NaBH_4$ with ultrasonication irradiation in the presence of hydroxyl-functionalized tetraalkyl ammonium chloride (**8**).[92] The produced Ir nanoparticles (IrNPs) were active for the biphasic hydrogenation of arenes. Hydroxyl-functionalized tetraalkyl ammonium chloride-protected Pd nanoparticles were prepared from Na_2PdCl_4 and used for Suzuki coupling reactions and the hydrogenation of halogenoarenes to arenes.[93,94] Reduction of Na_2PdCl_4 with 4-dimethylaminopyridine (DMAP, **11**) generated Pd nanoparticles that are active for the deuteration of pyridine derivatives.[95]

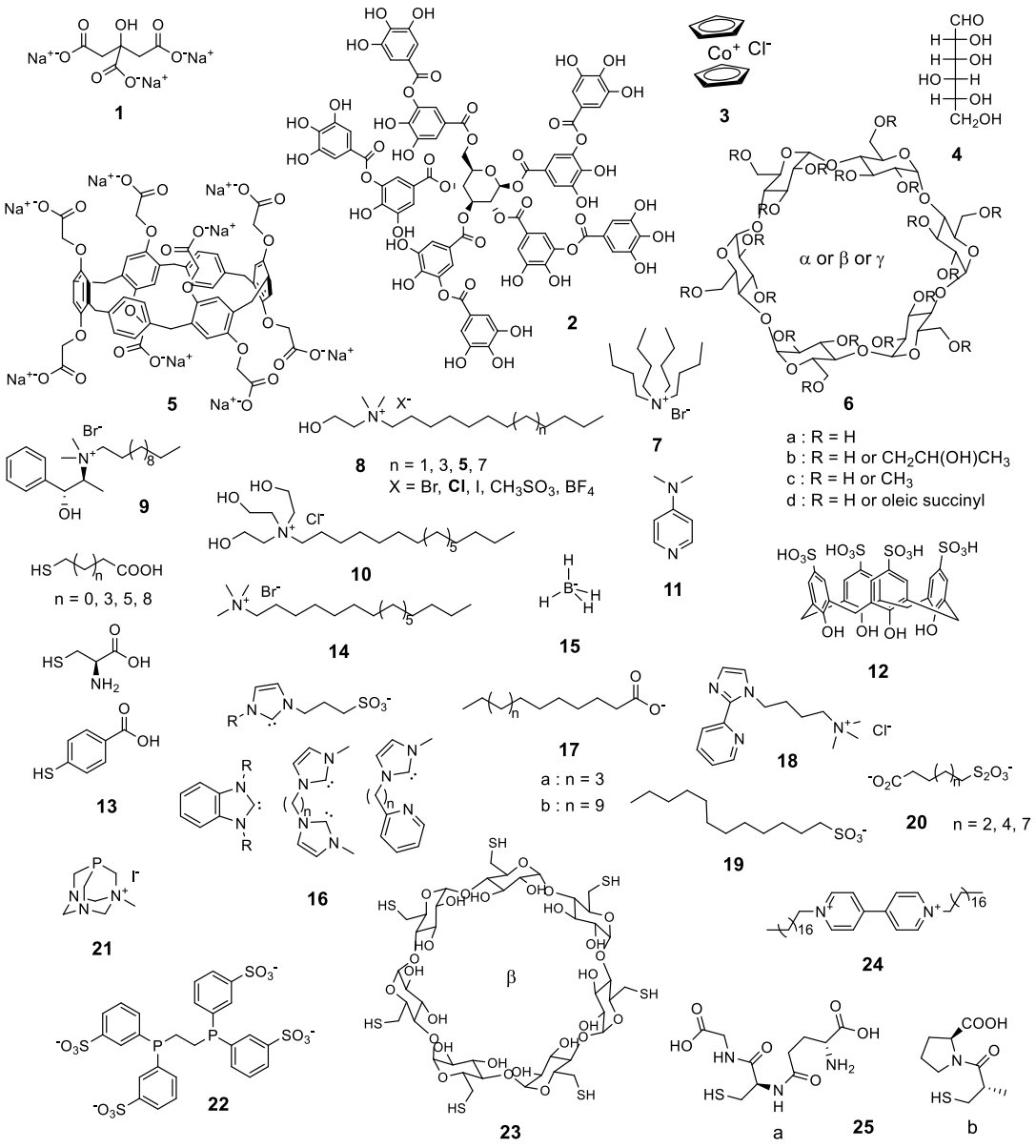

Figure 1. Organic ligands used for the stabilization of various metal nanoparticles soluble in water.

Thiol-based reagents are also often used for the synthesis of metal nanoparticles using $NaBH_4$ reduction of metal salts. Ru nanoparticles were prepared from $RuCl_3$ with $NaBH_4$ reduction in the presence of 4-sulfocarlixarenes (**12**) and could reduce brilliant yellow azo dye.[96] Various Au nanoclusters (Au_{25}) capped with different hydrophilic alkane- or arenethiols (**13**)

were prepared by direct $NaBH_4$ reduction and exhibited catalytic activities for the reduction of 4-nitrophenol.[97] Cetyltrimethyl ammonium bromide (**14**)-capped Au nanoparticles prepared by $NaBH_4$ reduction could be further grown into Au nanorods by slow reduction of $HAuCl_4$ using ascorbic acid.[64] These Au nanorods turned out to be an useful catalyst for selective hydrogenation of 4-nitrobenzaldehyde to 4-nitrobenzylalcohol. Direct reduction of several metal salts by $NaBH_4$ without any other stabilizing ligands has also been successful in preparing catalytic metal nanoparticles including Pd, Pt, Ag, and Au nanoparticles.[98,99] These nanoparticles are considered bare metal nanoparticles but the presence of electrostatic stabilization by borohydride (**15**) is likely the main reason for colloidal stability of metal nanoparticles. These metal nanoparticles have been investigated for the reduction of 4-nitrophenol.

H_2 has often been used as a reducing agent for the generation of metal nanoparticle catalysts. The advantage of H_2 reduction is the ease of purification due to the gases nature of the reducing agent. In comparison, $NaBH_4$ reduction resulted in the formation of boronic acids in water and often required a dialysis to remove this by-product. Sulfonated N-heterocyclic carbene (NHC, **16**)-stabilized Ru nanoparticles could be synthesized from Ru(COD)(COT) by using H_2 reductant.[100] This Ru nanoparticle showed an excellent activity for C-H deuteration of L-lysine. Ru nanoparticles could also be produced by reducing $[RuCl_2(p\text{-cymene})]_2$ with H_2 gas in the presence of imidazolium N-heterocyclic carbene (NHC, **16**) as a capping ligand.[101] Reduction of H_2PtCl_6 by H_2 in the presence of hydroxyl-functionalized tetraalkyl ammonium chloride (**9**) was able to successfully produce Pt nanoparticles that are tested for asymmetric hydrogenation of ethylpyruvate.[102]

Dimethylamine-borane is another reducing agent that could effectively reduce metal salts directly in organic medium (dimethylamine). Laurate (**17a**)-stabilized Ru and Rh nanoparticles

are synthesized from $RuCl_3$ and $RhCl_3$, respectively, and tested for the hydrolysis of ammonia-borane.[103,104] Various amines alone could be used as reducing agents for the direct reduction of metal salt precursors to metal nanoparticles in the presence of high thermal energy. For example, hexamethylrenetetraamine formed aldehyde ammonia that could reduce $PdCl_2$ to Pd nanoparticles capped with oleate (**17b**).[105] The Pd nanoparticles were found to be effective for dechlorination of aryl chloride and Suzuki coupling reactions. Tri-n-butylamine was used for the synthesis of Pd nanoparticles by reducing $PdCl_2$ and $Pd(OAc)_2$ at 80-120 °C.[106] The Pd nanoparticles were stabilized by tetrabutylammonium bromide (**7**) and could be used for in situ chemoselective hydrogenation of olefins and hydrolysis of epoxides in the presence of other functional groups such as carbonyl, aryl halide, and ether in water. Tetraalkylammonium halide (**7** and **18**)-protected Pd nanoparticles showing strong activity for Suzuki-Miyaura coupling reactions could also be prepared by reducing $Pd(COD)Cl_2$ with ammonia (NH_3) at 120 °C.[107]

Other miscellaneous direct reduction methods include the reduction of Na_2PdCl_4 by bromide at 100 °C in water and K_2PdCl_4. Bromide reduced Pd nanoparticles are capped with sodium dodecylsufate (SDS, **19**) and active for Suzuki coupling reaction.[108]

Table 1. Water-soluble Metal Nanoparticle (Ru, Rh, Pd, Ag, Ir, Pt, and Au) catalysts Synthesized by Direct Reduction in Water.

Catalysts	Ligand Stabilizers	Other Reagents	Ave Core Sizes & Notes	Reference
Ag NP	Citrate (**1**)	$AgNO_3$	10-200 nm	63
Au NP	Citrate (**1**)	$HAuCl_4$	18 nm	64
Au NP	Citrate (**1**)	$HAuCl_4$ $NaBH_4$	5 nm – 15 nm	65, 66, 67
Ag@Pd NP	Citrate (**1**)	K_2PdCl_4, $AgNO_3$ $NaBH_4$	10 nm Pd deposit on Ag	68

			NP	
Ag NP	Citrate then Tannic acid (**2**)	$AgNO_3$	10-200 nm Ligand exchange	63
Au NP	Tannic acid (**2**)	$HAuCl_4$	18-35 nm Au NP deposited on GO (12-33 nm)	70
Rh NP	Cobaticinium chloride ($[CoCp_2]Cl$) (**3**)	$RhCl_3$	1.3 nm Cobaltocene is an active reductant Rh NP on GO	71
Pd NP	Glucose (**4**)	$Pd(OAc)_2$	15 nm	72
Au NP	Anionic water-soluble leaning pillar[6]arene (AWLP6) (**5**)	$HAuCl_4$	11 nm	73
Au NP	α-Cyclodextrin (**6a**)	$HAuCl_4$ Basic sol. at 60 °C	10-50 nm	74
Pd NP	Hydroxypropyl-α-cyclodextrin (HP-CD) (**6b**)	$PdCl_2$	2-7 nm	75
Pd NP	Tetrabutylammonium bromide (TBAB) (**7**)	$PdCl_2$ 80 °C 100 °C Ultrasonic irradiation	2-6 nm Bromide is an active reductant 20-50 nm Size – N.A.	76 77 78
Rh NP	Hydroxyl-functionalized tetraalkyl ammonium bromide (HTAB) (**8**)	$RhCl_3$ $NaBH_4$	3.6 nm 2-2.5 nm Size – N.A.	79 80 81
Ru NP	Hydroxyl-functionalized tetraalkyl ammonium chloride (HTAC) (**8**)	$RuCl_3$ $NaBH_4$	2.5-3.5 nm 4 nm	82 83
Rh NP	Hydroxyl-functionalized tetraalkyl ammonium chloride (HTAC) (**8**)	$RhCl_3$ $NaBH_4$	2.7 nm	84
Rh NP	Hydroxyl-functionalized tetraalkyl ammonium w/ various anions (HTAX) (**8**)	$RhCl_3$ $NaBH_4$	2-2.5 nm 2-6 nm	85 86
Ru NP	Methylated-α or β or γ-	$RuCl_3$	1.5 nm	87

	cyclodextrin (Me-CD) (**6c**)	$NaBH_4$	2.5 nm 4 nm	88 83
Rh NP	N-Methylephedrium salts (**9**)	$RhCl_3$ $NaBH_4$	2.5 nm	89
Rh NP	Polyhydroxylated tetraalkyl ammonium chloride (PHTAC) (**10**)	$RhCl_3$ $NaBH_4$	3 nm	90
Ru NP	Oleic succinyl β-cyclodextrins (OS-β-CD) (**6d**)	$Ru(NO)(NO_3)_3$ $NaBH_4$	2.6 nm	91
Ir NP	Hydroxyl-functionalized tetraalkyl ammonium chloride (HTAC) (**8**)	$IrCl_3$ $NaBH_4$	1.9 nm Ultrasonic irradiation	92
Pd NP	Hydroxyl-functionalized tetraalkyl ammonium chloride (HTAC) (**8**)	Na_2PdCl_4 $NaBH_4$	2.7 nm Size – N.A.	93 94
Pd NP	4-Dimethylamino-pyridine (DMAP) (**11**)	Na_2PdCl_4 $NaBH_4$	3.4 nm	95
Ru NP	4-Sulfocarlix[4]arenes (**12**)	$RuCl_3$ $NaBH_4$	5 nm	96
Au NC	Hydrophilic alkane- and arene-thiols (**13**)	$HAuCl_4$ $NaBH_4$	1 nm – Au_{25}	97
Au nanorods	Cetyltrimethyl-ammonium bromide (CTAB) (**14**)	$HAuCl_4$ $NaBH_4$ and ascorbic acid	~20 nm + ~40 nm (width + length)	64
Ag NP	Bare – likely Borohydride (**15**)	$AgNO_3$ or $AgClO_4$ $NaBH_4$	Size – N.A.	98
Pd, Pt, and Au NP	Bare – likely Borohydride (**15**)	Na_2PdCl_4, H_2PtCl_6, and $HAuCl_4$ $NaBH_4$	3-5 nm	99
Ru NP	Sulfonated N-heterocyclic carbene (NHC) (**16**)	Ru(COD)(COT) H_2	1.5 nm COD: 1,5-cyclooctadiene COT: 1,3,5-cyclooctatriene	100
Ru NP	Imidazolium N-heterocyclic carbene (NHC) (**16**)	$[RuCl_2(p\text{-cymene})]_2$ H_2	4 nm	101
Pt NP	Hydroxyl-functionalized tetraalkyl ammonium	H_2PtCl_6 H_2	2.5 nm	102

	chloride (HTAC) (**8**)			
Ru NP	Laurate (**17a**)	$RuCl_3$ Dimethylamine-borane	2.6 nm	103
Rh NP	Laurate (**17a**)	$RhCl_3$ Dimethylamine-borane	5.2 nm	104
Pd NP	Oleate (**17b**)	$PdCl_2$ Hexamethylene-tetraamine	3.8 nm Aldehyde ammonia is an active reductant	105
Pd NP	Tetrabutylammonium bromide (TBAB) (**7**)	$Pd(OAc)_2$ Tri-n-butylamine 80 °C	Size – N.A.	106
Pd NP	Pyrydyl imidazole-functionalized tetraalkylammonium chloride (**18**) and tetrabutyl ammonium bromide (**7**)	$Pd(COD)Cl_2$ NH_3 120 °C	3 nm	107
Pd NP	Sodium dodecylsulfate (SDS) (**19**)	Na_2PdCl_4 100 °C	6-8 nm Halide is an active reductant	108

2.2. Phase Transfer from Organic to Aqueous Phases

It is most ideal to use water as a solvent for the synthesis of water-soluble metal nanoparticles. However, there are a few examples using the phase transfer strategy to prepare water-soluble metal nanoparticles for the purpose of improving the activity or selectivity of metal nanoparticle catalysts (Table 2). For example, water-soluble ligand capped Pd nanoparticles were synthesized via the thiosulfate method using ω-carboxyl-S-alkyl thiosulfate (**20**) as the ligand.[109-111] The synthesis involves a two-phase system in order to prevent the hydrolysis of the thiosulfate ligand. A schematic representation of the alkyl thiosulfate protocol is shown in Scheme 2. The synthesis involves the complete transfer of $PdCl_4^{2-}$ (Pd^{2+}) and alkyl thiosulfate ligand from the aqueous layer to the organic layer of the solution using phase transfer agent, tetraoctylammonium

bromide (TOAB). Next, the reduction of the palladium metal Pd^{2+} to Pd^{0} is achieved with the use of sodium borohydride ($NaBH_4$) as the reducing agent. Immediately after the addition, the palladium atoms begin to nucleate into the desired nanosized particles in organic phase. At the end of the procedure, the Pd nanoparticles capped with carboxylate-terminated alkanethiolate ligands are phase transferred back in to the aqueous phase. Previous studies from the Shon group have shown that the size and ligand surface coverage of the PdNPs can be controlled by adjusting the amounts of TOAB, $NaBH_4$, and ligand used. It was noticed that a reduction in the molar equivalent amount of $NaBH_4$ led to a decrease in the surface ligand density and an increase in the core size of the nanoparticle. In addition, shorter chained ligands (ω-carboxyl-S-hexyl thiosulfate (C6) vs ω-carboxyl-S-undecyl thiosulfate (C11)) led to a decrease in the surface ligand density under the same condition.[109] This decrease can be attributed to a higher polarity of C6 ligands and a stronger kinetic impediment by TOAB. These water-soluble palladium nanoparticles were tested for their catalytic activity for hydrogenation and isomerization reactions of allylic alcohols and acetylenes.[109-111] Overall, a higher catalytic activity was observed for water-soluble nanoparticles that had a lower surface coverage. Similarly, the phase transfer of TOAB-capped Pd nanoparticles by replacing TOAB with water-soluble aminophosphine ligands (**21**) allowed the catalytic investigation of water-soluble Pd nanoparticles for the hydrogenation of alkynes and alkenes in biphasic conditions.[112]

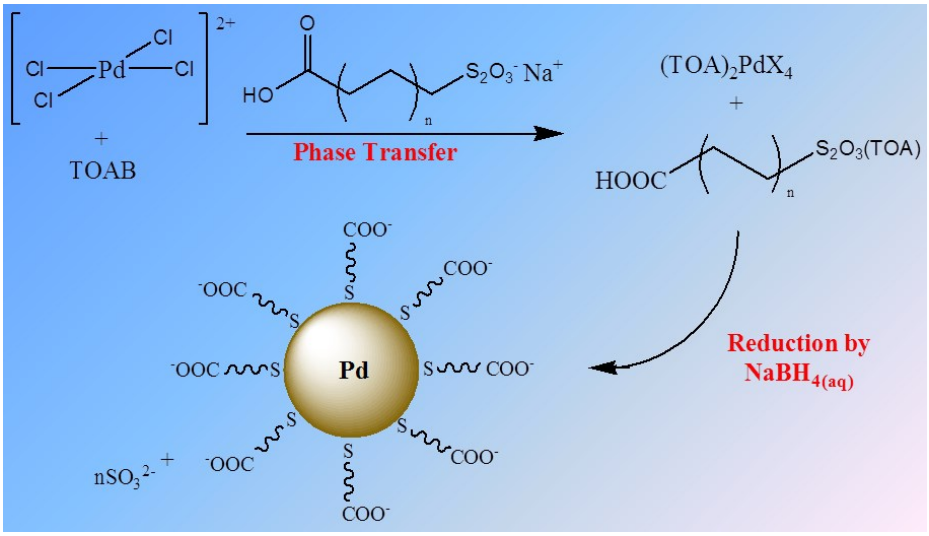

Scheme 2. Reaction scheme for the two-phase synthesis of water-soluble palladium nanoparticles generated from ω-carboxyl-*S*-alkanethiosulfate salts [Reproduced with the permission of ref (109). Copyright 2013 American Chemical Society].

2.3. Redispersion of Nanoparticles in Water

When one or more reagents necessary for the synthesis of metal nanoparticles exhibit a poor solubility in neat water, another solvent that can act as a better solubilizing solvent and at the same time can be homogeneously mixed with water is used (Table 2). Once the synthetic reactions are completed, however, the entire organic or mixed aqueous solvents are removed completely before the metal nanoparticles are redispersed or redissolved in pure water. For example, Ru[(COD)(COT)] dissolved in THF was reduced and grown to Ru nanoparticles in the presence of H_2, the reducing agent, and alkyl sulfonated diphosphine (**22**), the capping agent.[113] The solvent THF was removed by vacuum evaporation and the Ru nanoparticles are redissolved in water for the catalytic hydrogenation of alkenes and carbonyls. For the synthesis of thiolated cyclodextrin (**23**)-capped Pd nanoparticles investigated for the catalytic reactions including the hydrogenation of alkenes and Sonogashira coupling reaction, the mixed solvent systems such as

DMSO-water or DMF-water were used for the reduction of Na_2PdCl_4 by $NaBH_4$.[114-116] The same work was also reported for the synthesis of thiolated cyclodextrin (**23**)-capped Pt nanoparticles from Na_2PtCl_4.[114] Pt nanoparticles produced after the reduction of H_2PtCl_6 by viologen in DMF-water and stabilized by octadecyl viologen (**24**) could be studied for the reduction of 4-nitrophenol in water.[117] Glutathione (**25a**) or captopril (**25b**)-capped Au nanoparticles could be synthesized in methanol-water co-solvent system after the reduction of $HAuCl_4$ by $NaBH_4$ and investigated for the chemoselective hydrogenation of 4-nitrobenzaldehyde.[118]

Table 2. Water-soluble Metal Nanoparticle (Ru, Pd, Pt, and Au) catalysts Synthesized by Other Methods: Phase Transfer and Redispersion of Nanoparticles.

Catalysts	Ligand Stabilizers	Other Reagents	Ave. Core Sizes and Notes	References
Pd NP	ω-carboxylate-S-alkyl thiosulfate (**20**)	K_2PdCl_4 $NaBH_4$ TOAB Toluene/water	1.7 – 1.9 nm Phase transfer Pd NP w/ GO	109, 110 111
Pd NP	Water-soluble aminophosphine (e.g. 1,3,5-triaza-7-phosphaadamantane) (**21**)	K_2PdCl_4 $NaBH_4$ TOAB	2.8-3.5 nm Phase transfer	112
Ru NP	Alkyl sulfonated diphosphines (**22**)	Ru[(COD)(COT)] H_2 THF/water	1.2-1.5 nm Re-dispersion	113
Pd and Pt NP	Thiolated-β cyclodextrins (**23**)	Na_2PdCl_4 and Na_2PtCl_4 $NaBH_4$ DMSO/water	16 nm and 14 nm Re-dispersion	114
Pd NP	Thiolated-β-cyclodextrin (**23**)	Na_2PdCl_4 $NaBH_4$ DMSO/water DMF	3 nm Re-dispersion 3 nm Re-dispersion	115 116
Pt NP	Octadecyl viologen micelles (**24**) (Pt NP-viologen micelle hybrids)	H_2PtCl_6 Viologen DMF/water	1 nm Re-dispersion	117

Au NC	Glutathione (**25a**) Captopril (**25b**)	$HAuCl_4$ $NaBH_4$ Methanol/water	1-1.5 nm $Au_n(SR)_m$ Re-dispersion	118

3. ORGANIC REACTIONS OF NOVEL METAL NANOPARTICLES IN WATER

3.1. Hydrogenation of Unsaturated Hydrocarbons

Hydrogenation reactions confer the treatment of organic compounds having unsaturated π bonds with the addition of molecular hydrogen to transform into saturated or reduced species. Catalysts are typically a necessary component in hydrogenation reactions to having taken place at the milder conditions such as lower temperature. Catalytic hydrogenation reaction plays a vital role in the development of various kinds of consumer products, from food to pharmaceutical industries.[119] There are numerous reports that have been published on synthesis, characterization, and utilization of water-soluble metal nanoparticles with various sizes and stabilizing ligands as an efficient catalyst for the hydrogenation of unsaturated hydrocarbons (Table 3).

3.1.1. Cyclodextrin-capped metal nanoparticles

One of the earlier work reported by Kaifer et al. has shown that water-soluble thiolated-β-cyclodextrin-stabilized PdNPs (~16 nm) and PtNPs (~14 nm) act as homogeneous catalysts for hydrogenation of allylamine (136 μL, 1.8 mmol) to 1-propylamine at room temperature under 1 atm of H_2 pressure.[114] The results indicated that 95-100 % conversion is achieved by 10 mg of each catalyst after 6 hr. However, 5 mg of Pt and PdNPs were able to achieve only 10 and 30 % conversions, respectively.

Thiolated-β-cyclodextrin-stabilized PdNPs (β-CD/Pd) with an average diameter of 3 nm were later illustrated for the hydrogenation of various hydrophobic substrates in an aqueous biphasic system.[115] It was found that the hydrogenation of C=C bond in conjugated carbonyl compounds such as 3,3,5-trimethyl-2-cyclohexenone (isophorone) occurs at the faster rate (e.g. 100 % in aqueous biphasic condition within 2 hours with a TOF of 26 h^{-1} vs 25 % in ethanol). Most alkene substrates were hydrogenated within 2-5 hours with the conversion rates ranging from 70 – 100 % under similar reaction conditions. A control study using Pd black catalyst, in comparison, resulted in 100 % conversion of isophorone in ethanol but only 2 % in water. TOF data shown in Figure 2 indicated that the addition of free β-CD does not enhance the efficiency of this catalytic hydrogenation. It was proposed that the presence of hydrophobic CD cavities in aqueous media promotes the host-guest complexation of hydrophobic substrates with surface-bound β-CD and increases the rate of conversion.

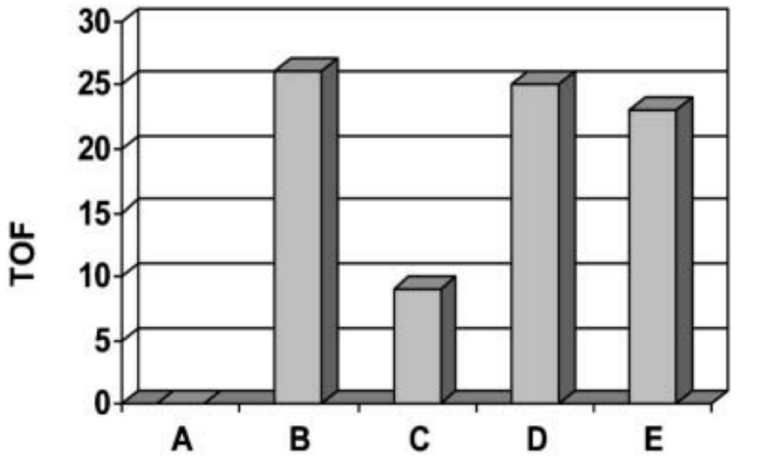

Figure 2. Relative turnover frequency (TOF, h^{-1}) as compared with Pd black (A) for the hydrogenation of isophorone (1 mmol) in the presence of 10 mg of catalyst in aqueous biphasic media. (A) Pd black, 0.1 h^{-1}; (B) β-CD/Pd, 26 h^{-1}; (C) β-CD/Pd + 1 mmol of adamantane, 9 h^{-1};

(D) β-CD/Pd + 1 mg of free β-CD, 25 h^{-1}; (E) β-CD/Pd + 10 mg of free β-CD, 23 h^{-1} [Reproduced with the permission of ref (115). Copyright 2005 Royal Society of Chemistry].

The efficiency of methylated cyclodextrins (Me-CDs), which are without functional groups that bind to surface strongly, on stabilizing RuNPs during the catalytic reactions was soon demonstrated.[88] The molar ratio of Me-CDs over Ru (R = Me-CD/Ru) was varied and its effects on the stability of RuNPs was investigated. RuNPs at R = 10, 30, and 50 could maintain visually stable dispersed states and were without any trace of sedimentation, but RuNPs at R = 3 and 5 started to show the clear signs of aggregation during and after the reactions. Me-CDs-stabilized RuNPs at R = 10 exhibited the highest catalytic activity for the hydrogenation of 1-dodecene to dodecane and were investigated for the catalytic hydrogenations of various olefins and alkynes under biphasic conditions. Me-CDs with various shapes (α, β, γ) and different degrees of methylations were compared for understanding the effects of cavity size and hydrophobicity. TOF results remained similar regardless of the cavity size and the methylation degree of Me-CDs. There are a slight decrease in TOF values as alkyl chain lengths of the olefins increase (C10 > C12 > C14). This phenomenon was attributed to the decrease in the water solubility of the cyclodextrin/olefin inclusion complexes with the increase in alkyl chain length of the olefins. The reactions with aromatic alkenes such as styrene resulted in the chemoselective hydrogenation of alkene group in the presence of arene moiety. This indicated the modulating property of Me-CDs on arene hydrogenation activity of RuNPs. The hydrogenation of pinenes (α and β) in the presence of Me-CDs-stabilized RuNPs produced the diastereomeric cis-pinanes as major products exhibiting the stereospecific potentials of RuNPs.

In a recent report, oleic succinyl-β-cyclodextrin-stabilized RuNPs (Ru_OS-β-CD) was applied for aqueous hydrogenation of olefins.[91] The well-dispersed particles were found to have

a narrow size distribution with an average diameter of 2.6 nm. The zeta potential of Ru_OS-β-CD NPs was calculated to be -40 mV, indicating its good stability in the aqueous colloidal suspension. The reaction time for aqueous hydrogenation of terminal olefins (1-octene, 1-decene, and 1-tetradecene) was significantly increased with the increased alkyl chain lengths of the olefin substrates. This result again supported that the solubility of the cyclodextrin/olefin inclusion complexes has a great influence on the hydrogenation activity of RuNPs.

3.1.2. Tetraalkylammonium ions-capped metal nanoparticles

Tetra-*N*-butylammonium bromide (TBAB, n-Bu_4NBr)-protected water-soluble palladium nanoparticle catalyst was explored for the catalytic hydrogenation of the functionalized alkenes.[120] The results indicated that the C=C of various conjugated carbonyls and allyl aromatic compounds could be hydrogenated chemoselectively in the presence of halide, epoxide, carbonyl, ester, nitrile, and benzylic ether groups with the high conversion rates in aqueous media.

3.1.3. Phosphine-capped metal nanoparticles

Alkyl sulfonated diphosphine-stabilized RuNPs could be used for the hydrogenation of 1-tetradecene and styrene in biphasic liquid-liquid environments at both atmospheric and high pressure conditions.[113] The NPs were water dispersible with the size in the range of 1.2 – 1.5 nm as well as in the form of well-crystallized nanoclusters with hydride moiety on the surface. The conversion of styrene into ethylbenzene took place under atmospheric condition with the reaction time of 1 hr. In contrast, the hydrogenation of 1-tetradecene was very slow because of solubility problem in water. A higher temperature and longer reaction time (40 hr) were necessary to reach 100 % conversion of 1-tetradecene.

Water-dispersible PdNPs stabilized by the hydrophilic aminophosphine ligands including 1,3,5-triaza-7-phosphaadamantane (PTA) were investigated for the catalytic hydrogenation of alkynes, alkenes, and dienes under mild conditions (20 °C and H_2 pressure of 1-10 bar) in biphasic media.[112] The performance of catalytic hydrogenation of the Pd@PTA NPs was entirely dependent on the Pd/PTA ratio. It was observed that Pd@PTA (1:1) with lower ligand density was more effective towards the reduction of hydrophobic alkenes such as 1-dodecene (TOF = 257 h^{-1}) and alkynes such as diphenylacetylene (TOF = 360 h^{-1}). In contrast, Pd@PTA (1:4) with a higher ligand ratio could not perform the conversion of 1-dodecane (TOF = 4.2 h^{-1}) and diphenylacetylene (TOF = 41.6 h^{-1}) in similar fashion. The outcomes indicated the low accessibility of substrates to the PdNP surface with higher ligand density. Recyclability of the particles in aqueous environment were performed and the results indicated that Pd@PTA was capable of maintaining the complete hydrogenation conversions up to 9 cycles.

3.1.4. Alkylthiolate-capped metal nanoparticles

The catalytic properties of water-soluble ω-carboxyl-1-hexanethiolate-capped PdNPs (C6-PdNP) and ω-carboxyl-1-undecanethiolate-capped PdNP (C11-PdNP) synthesized using sodium ω-carboxyl-S-alkanethiosulfate ligand precursors were explored for the hydrogenation of allyl alcohol in D_2O.[109] The homogeneous reaction of C6-PdNP was reported to be more effective than that of C11-PdNP. The reaction with C6-PdNP has yielded ~91% of 1-propanol and ~5% of propanal with TOF of 455 h^{-1} after 4 hr reaction. Lower surface ligand coverage and the shorter ligand chain length has provided less steric hindrance for the formation of linear Pd-alkyl intermediate and the hydrogenation product. The increase in H_2 gas (10 mmol) concentration could further increase the yields of 1-propanol to 98% (2% propanol) with TOF of 490 h^{-1}. The results reflected that the longer hydrophobic chain of surface ligand makes C11-PdNP

comparably less polar and decreases the solubility and catalytic activity in an aqueous environment (58 % 1-propanol and 11% propanal with TOF of 290 h^{-1}).

Catalytic activity and selectivity of the micellar water-soluble C6-PdNP and ω-carboxyl-1-octanethiolate-capped PdNP (C8-PdNP) for the biphasic hydrogenation and isomerization of hydrophobic allylic alcohols with long alkyl chains were also investigated.[110] A complete conversion of 1-octen-3-ol to either hydrogenation (73%) or isomerization (27%) products by C6-PdNP was only observed after 24 hr reaction when at least 10 mol% of PdNP (in Pd mol%) and excess H_2 gas were introduced to the reaction mixture. The activity and selectivity was found to be impacted by the pH of nanoparticle solution. A slow conversion of 1-octen-3-ol to either hydrogenation or isomerization products was observed (only 15-30%) at lower pH (2-6) because of the poor solubility of C6-PdNP in acidic solution. In contrast, complete conversion was observed after 24 hr with the formation of both hydrogenation and isomerization products in 73:27 ratio at pH 7, indicating the increase in both activity and selectivity towards the hydrogenation at higher pH. However, no significant changes in both activity and selectivity of the catalytic reactions were observed when the pH of the solution was further increased to pH 10. The catalytic reactions of 1-octen-3-ol, 1-nonen-3-ol, and 1-decen-3-ol by both the C6-PdNP and C8-PdNP indicated that more hydrogenation over isomerization products were obtained from 1-octen-3-ol and 1-nonen-3-ol, but opposite results were observed from 1-decen-3-ol. The increase in the substrate-ligand interaction of 1-decen-3-ol with hydrophobic alkyl chains was suggested as the potential cause for different selectivity.

The effects of colloidal graphene oxides on the catalytic activity and selectivity of water-soluble C6-PdNP for alkyne hydrogenation reaction of dimethyl acetylene dicarboxylate (DMAD) were investigated.[111] The kinetic plots of the catalytic hydrogenation of DMAD by

PdNP and PdNP/GO catalysts indicated that these catalysts are more selective towards the semi-hydrogenation product. Most DMAD was hydrogenated to the semi-hydrogenated product (maleic ester) in a cis-form (>99% selectivity) in less than 3 h of reaction time. The TOF values for semi-hydrogenation products by PdNP and PdNP/GO were 916 and 871 h^{-1}, respectively. This observation indicated that the GO did not have a significant effect on the overall activity and selectivity toward semi-hydrogenation at room temperature and atmospheric pressure. However, the overall colloidal stability of PdNP/GO was significantly higher than that of PdNP alone (Figure 3).

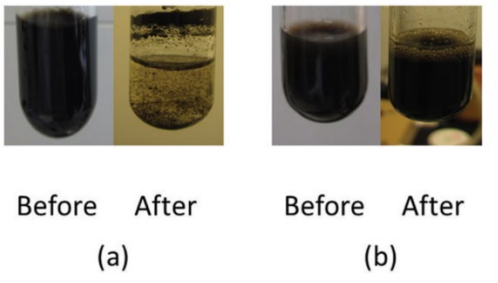

Figure 3. Reaction systems before and after 24-hour DMAD hydrogenation reactions with (a) PdNPs and (b) PdNP/GO [Reproduced with the permission of ref (111). Copyright 2017 Royal Society of Chemistry].

Table 3. Hydrogenation of Unsaturated Hydrocarbons Catalyzed by Novel Metal Nanoparticles in Water.

Catalysts	Ligand Stabilizers	Catalytic Reactions	Catalysis Notes	References
Pd and Pt NP 16 nm and 14 nm	Thiolated-β cyclodextrins (**23**)	Hydrogenation of allyl amine (monophasic)	100 %	114
Pd NP 3 nm	Thiolated-β cyclodextrins (**23**)	Hydrogenation of alkenes (biphasic)	100% (26 h^{-1}) 5 recycles	115
Ru NP 2.5 nm	Methylated-α or β or γ-cyclodextrin (Me-CD)	Hydrogenation of alkenes and alkynes (biphasic)	17 to 69 h^{-1} rt, 1 atm H_2	88

	(**6c**)			
Ru NP 2.6 nm	Oleic succinyl β-cyclodextrins (OS-β-CD) (**6d**)	Hydrogenation of olefins (biphasic)	100 % hydrogenation in 60 – 3800 min using 1 mol% Ru	91
Pd NP 4.1 nm	Tetrabutylammonium bromide (TBAB) (**7**)	In situ chemoselective hydrogenation of olefins (biphasic)	90-98% > ester, benzylic ether, carbonyl, nitrile, aryl halide, epoxide	120
Ru NP 1.2-1.5 nm	Alkyl sulfonated diphosphines (**22**)	Hydrogenation of alkenes (biphasic)	Up to 100 %	113
Pd NP 2.8-3.5 nm	Water-soluble aminophosphine (e.g. 1,3,5-triaza-7-phosphaadamantane) (**21**)	Hydrogenation of alkynes and alkenes in (biphasic)	12-992 h^{-1} (99 % cis-pinane selectivity) 9 recycles	112
Pd NP 1.7 nm	ω-carboxylate-S- alkyl thiosulfate (**20**)	Hydrogenation of allyl alcohol (monophasic)	490 h^{-1}	109
Pd NP 1.8 nm	ω-carboxylate-S- alkyl thiosulfate (**20**)	Hydrogenation of allylic alcohols (biphasic)	77 % (10 mol% Pd)	110
Pd NP 1.9 nm Pd NP/GO 2.0 nm	ω-carboxylate-S- alkyl thiosulfate (**20**)	Hydrogenation of dimethyl acetylene dicarboxylate (monophasic)	916 h^{-1} semi (Pd NP) 871 h^{-1} semi (Pd NP/GO)	111

3.2. Hydrogenation of Aromatic Hydrocarbons

The presence of aromatic compounds in diesel has been known to decrease its overall fuel quality.[121] Carcinogenic nature of aromatic moieties has also made the emission of diesel in exhaust gases problematic for environments. In addition, the hydrogenation of aromatic compounds to cycloalkane and cycloalkene derivatives has been greatly important for both academics and industries. These are the main reasons that the hydrogenation of aromatic compounds using various metal catalysts including Pd, Ru, Rh, and Ir has been intensely

investigated with a focus on developing active nanoparticle catalysts that function at the mild conditions and in aqueous solutions (Table 4).[56]

3.2.1. Tetraalkylammonium ions-capped metal nanoparticles

Ruocoux and coworkers have first demonstrated the arene hydrogenation catalysis of RhNPs stabilized by an organic-ligand that could be synthesized from the reaction between *N,N*-dimethylethanolamine and 1-bromoalkanes.[79] They have synthesized four ligands with different alkyl chain lengths (C12, C14, C16, and C18) to stabilize RhNPs. The ligands containing C16 and C18 alkyl chains were found to produce more stable aqueous suspension of RhNPs. Colloidal C16-RhNP and C18-RhNP used for catalytic hydrogenation of benzene derivatives under biphasic conditions at room temperature and atmospheric pressure were also found to be more effective in producing corresponding cyclohexane derivatives with 100 % conversion rate. The reactions were completed within 5 to 10 hr with the TOF value in the range of 30 to 65 h^{-1}. It was observed that the presence of electron-donating substituents influence the reaction kinetics more positively than that of electron-withdrawing groups. In addition, the hydrogenation of disubstituted benzene derivatives such as o-xylene, m-xylene, and p-xylene produced both *cis*- and *trans*-dimethylcyclohexane with their *cis*-product being more favored.

In their subsequent report, the Roucoux group has further examined the stability of RhNPs stabilized by *N*-alkyl-*N*-(2-hydroxyethyl)ammonium salts (HEA with C14, C15, and C16).[80] The most stable C16-RhNP was used for catalytic hydrogenation of various arenes including benzene, anisole, phenol, ethyl benzoate, xylene, and cresol. Most substrates were completely converted to the corresponding cyclohexane products with TOFs between 37 and 67 h^{-1} except for bromobenzene, which was remain unreacted. It was concluded that the reaction

kinetics were influenced by the steric effects of the aromatic substituents as the reactions took longer for arenes with bulkier substituents. TOF values were, however, found to decrease when the catalysts were reused.

To further improve the catalytic activity and efficiency of C16-RhNP, the same group has investigated the role of surfactant concentrations during the catalytic reactions.[81] Surface tension measurements have revealed the self-aggregation nature of the surfactants into micelles above the critical micellar concentration (CMC) of 3.2 X 10^{-4} mol/L. The catalytic hydrogenation of various arenes in different surfactant concentrations revealed that the rate of hydrogenation becomes faster with higher TOF (up to 429 h^{-1}) when the surfactant concentrations are below the CMC.

The effects of the counter ions (X = Br, Cl, I, CH_3SO_3, BF_4) under the similar conditions were investigated using C16-RhNP with various anions (Br^-, Cl^-, I^-, $CH_3SO_3^-$, BF_4^-).[85] The size of the counter ions was found to affect the micelle formation and the CMC because larger counter-ions are more polarizable and contribute to decreasing electrostatic repulsions between head groups. Zeta potentials of C16-RhNP with various anions were measured to bear positive charges in solution in the range of 40 to 100 mV. Surface tension measurements confirmed the self-aggregation of HEA-C16 into micelles above the CMC of 1.1 x 10^{-3}, 1.4 x 10^{-3}, 9.3 x 10^{-4}, 1.3 x 10^{-5} and 2.8 x 10^{-4} mol/L for Br^-, Cl^-, I^-, $CH_3SO_3^-$, and BF_4^-, respectively. However, the particle size in the range of 2.1 to 2.4 nm of highly stable and monodispersed C16-RhNP was not affected by the size of the counter ions. The hydrogenation of benzene derivatives by C16-RhNP with different counter ions indicated that C16-RhNP with Cl^- exhibits the highest TOF value in complete conversions of substrates to corresponding cyclohexane derivatives. The studies on the hydrogenation of disubstituted benzene derivatives showed that the nature and the position of the

substituents have played some roles on affecting the reaction as the reactivity decreases in the order of para > meta > ortho position. The influence of hydrogen pressure indicated that the TOF values of anisole hydrogenation using C16-RhNP with Cl^- increases from 58 h^{-1} at 10 bar to 100 h^{-1} at 30 bar.

More diverse anions including HCO_3^-, F^-, BF_4^-, and $CF_3SO_3^-$ were further incorporated to C16-RhNP.[86] Interestingly, C16-RhNP with F^-, BF_4^-, and $CF_3SO_3^-$ exhibited worm-like shape or dendrites in aqueous media with an average diameter of about 3 nm. In comparison, isolated and spherical colloids were produced with Cl^- and HCO_3^- as counter anions. The catalytic reactions of benzene, toluene, anisole, and o-xylene using C16-RhNP at 20 bar of hydrogen pressure resulted in complete hydrogenations to corresponding cyclohexanes within 1 hr. The highest TOF value of benzene conversion at 3,600 h^{-1} indicated an excellent interaction of benzene with the aqueous suspension of the C16-RhNP catalyst (benzene > anisole > toluene > o-xylene). The lower solubility of other benzene derivatives like toluene, anisole, and o-xylene was proposed to negatively affect their catalytic conversions. In addition, the counter ions (HCO_3^-, F^-, BF_4^-, and $CF_3SO_3^-$) associated with the ammonium group were found to influence the reaction rate and TOF values (360 – 3600 h^{-1}) of the reactions.

Polyhydroxylated ammonium salt, *N*-hexadecyl-*N*-tris-(2-hydroxyethyl) ammonium chloride (THEA16Cl), were investigated for stabilization of RhNPs.[90] The monodispersed THEA16Cl-stabilized RhNP (Rh/THEA16Cl) was reported to have an average diameter of 3 nm. Hydrogenation of benzene derivatives in the presence of Rh/THEA16Cl indicated that benzene, toluene, and ethyl benzoate were completely converted to the corresponding cyclohexane derivatives with TOFs ranging from 86 to 300 h^{-1}. However, a side reaction was observed for anisole which was converted to methoxycyclohexane (78%) and cyclohexanone (22%) with TOF

value of 120 h^{-1}. Another modification on the surfactant structure were also attempted by changing hydroxyethyl group to hydroxypropyl group, *N,N*-dimethyl-*N*-cetyl-*N*–(3-hydroxypropyl) ammonium chloride (HPA16Cl).[122] The hydrodynamic diameters of Rh/HEA16Cl (8.8 nm), Rh/HPA16Cl (28.0 nm), and Rh/THEA16Cl (17.8 nm) were found to be increased according to the polar head of the surfactants. However, all the particles have generated positive charges in solution in the range of 40.5 to 58.4 mV. The overall reaction time for the hydrogenation of all substrates was in the range of 1 to 10 hr with the corrected TOFs in the range of 75 to 750 h^{-1}. The analysis indicated that Rh/THEA16Cl was most effective towards the catalytic reactions with the higher TOF of >300 h^{-1}. In contrast, the lowest activity was observed from Rh/HPA16Cl with the TOF of <90 h^{-1}. The results indicated that the larger hydrodynamic size of HPA16Cl might have caused the catalyst less accessible to the substrate.

The catalytic studies of iridium nanoparticles stabilized by HEA16Cl (Ir/HEA16Cl) have also appeared in the literature.[92] Most arenes were completely hydrogenated to the corresponding cyclohexane derivatives within 2 hr with TOFs of 100 - 400 h^{-1}. As seen from the catalysis of RhNP, the reaction rate for the hydrogenation of arenes by IrNP was affected by steric and electronic effects of substituents as electron-withdrawing groups slow down the reaction, whereas electron-donating substituents enhance the rate. It was reported that the aqueous suspension of IrNP was reusable for 3 consecutive runs with similar TOF.

HEA16Cl-stabilized RuNPs (Ru/HEA16Cl) were reported for the hydrogenation of arenes in biphasic liquid-liquid (water/hydrocarbon) systems at room temperature under 30 bar of hydrogen pressure.[82] Complete conversion from the hydrogenation of benzene and mono-alkylated benzene was demonstrated within 2 h of reaction in the presence of Ru/HEA16Cl without the formation of any visible aggregation of the catalyst. The effects of the magnetic

stirring (1,500 min^{-1}) and gas projection impeller (GPI) (1,000 min^{-1}) were discussed. Especially the presence of a gas projection impeller during the catalytic reaction of benzene resulted in about four times higher TOF (600 h^{-1}) than that of reactions with just magnetic stirring (150 h^{-1}). It was also shown that the hydrogenation of substituent arenes including styrene, anisole, and acetophenone completes under GPI after 1.5, 1, and 3.5 hrs with TOFs of 266, 300 and 150 h^{-1}, respectively. In the case of o-xylene, the complete conversion was occurred to produce *cis* and *trans* derivatives with a major formation of the *cis*-diastereoisomer (95%).

3.2.2. Cyclodextrin-capped metal nanoparticles

Moniflier group has reported aqueous suspension of RuNPs stabilized by 1:1 inclusion complexes formed by blending HEA16Cl and methylated cyclodextrins (Me-β-CD).[83] The synthesized Me-β-CD/HEA16Cl-stabilized RuNPs exhibited the better catalytic activity for the hydrogenation of arenes compared to RuNP stabilized by individual HEA16Cl or Me-β-CD. It was found that styrene completely converts to ethyl benzene with TOF of 83.3 h^{-1}, but anisole and toluene are hydrogenated to methoxy cyclohexane and methyl cyclohexane, respectively, in ~80 % with TOF value of ~10 h^{-1}.

The difference in activity of RuNPs stabilized with methylated cyclodextrins with different sizes (Me-α-CD, Me-β-CD, and Me-γ-CD) was investigated to understand the effects triggered by differing interactions between substrates and cyclodextrins.[87] Methylated-cyclodextrins (Me-α-CDs)-stabilized RuNPs could not catalyze the hydrogenation of benzene, styrene, and ethyl benzene under the mild conditions. In contrast, Me-γ-CD/RuNPs have unveiled 100% conversions for the same substrates with TOFs at 4 – 10 h^{-1}. In the case of Me-β-CD/Ru NPs, the hydrogenation of arenes was occurred according to substitution degree, which

was defined as the average number of hydroxyl groups substituted per glucopyranose unit in Me-CD.[88] When Me-β-CD has low substitution degree (0.7), various benzene derivatives would undergo full hydrogenation. In contrast, only benzene and toluene were hydrogenated at higher substitution degree (1.8) whereas aromatic rings having an alkyl chain of more than two carbons such as styrene, ethyl benzene, and propyl benzene were not hydrogenated.

Oleic succinyl-β-cyclodextrin stabilized RuNPs (Ru_OS-β-CD) was also applied for aqueous hydrogenation of various arenes.[91] Aqueous hydrogenation of styrene was completed within 1 hr at a temperature of 30 °C and a hydrogen pressure of 10 bar with a styrene/ruthenium molar ratio equal to 100. However, the catalytic system with a physical mixture of oleic acid sodium salt and β-CD along with RuNPs resulted in no conversion and became unstable. This observation hinted the efficiency of OS-β-CD on stabilizing Ru_OS-β-CD NP catalysts. Other aromatic compounds including anisole, allyl benzene, benzaldehyde, and benzyl alcohol were completely hydrogenated into their fully saturated equivalents within 20 hr. The efficiency of the catalyst was also confirmed on the biomass-based substrates such as citronellal, furfural, and furfuryl alcohol.

3.2.3. Phosphine-capped metal nanoparticles

The alkyl sulfonated diphosphine-stabilized RuNPs were investigated for the hydrogenation of styrene in biphasic systems at atmospheric and high pressure reaction conditions.[113] The conversion rate of styrene into ethyl benzene and/or ethyl cyclohexane during hydrogenation under atmosphere condition was found to vary depending on the reaction time and temperature. Results indicated that only 75% of ethyl benzene was produced without the formation of ethyl cyclohexane in the presence of RuNPs in the first hour. After 24 hr reaction, the selectively was

observed to be 45 % ethyl benzene and 55 % ethyl cyclohexane. The ethyl cyclohexane selectivity was increased to 97 % after 40 hr reaction with the ethyl benzene selectivity decreasing to 3 %. Styrene hydrogenation under 10 bar hydrogen pressure also resulted in similar time dependent results.

3.2.4. Organometallic ligand-capped metal nanoparticles

Water-soluble cobalticinium chloride-stabilized RhNP catalysts were reported to catalyze the hydrogenation of benzene to cyclohexane in aqueous media.[71] A supported RhNPs on reduced graphene oxide (RhNP/rGO) was also demonstrated for the same reaction. RhNPs and RhNP/rGO produced similar results for the hydrogenation of benzene with 99% conversion yields and TOFs of ~12.4 h^{-1} at slightly elevated temperature (40 °C).

Table 4. Hydrogenation of Aromatic Hydrocarbon Catalyzed by Novel Metal Nanoparticles dissolved in Water under Biphasic Conditions.

Catalysts	Ligand Stabilizers	Catalytic Reactions	Catalysis Notes	References
Rh NP 3.6 nm	Hydroxyl-functionalized tetraalkyl ammonium bromide (HTAB) (**8**)	Hydrogenation of arenes (biphasic)	30-65 h^{-1} rt, 1 atm H_2	79
Rh NP 2-2.5 nm	Hydroxyl-functionalized tetraalkyl ammonium bromide (HTAB) (**8**)	Hydrogenation of arenes (biphasic)	188 h^{-1} rt, 1 atm H_2	80
Rh NP Size – N.A.	Hydroxyl-functionalized tetraalkyl ammonium bromide (HTAB) (**8**)	Hydrogenation of arenes (biphasic)	149 - 429 h^{-1} at the surfactant concentration just below CMC	81
Rh NP 2-2.5 nm	Hydroxyl-functionalized tetraalkyl ammonium w/ various anions (HTAX) (**8**)	Hydrogenation of arenes (biphasic)	36 - 100 h^{-1} Effects of the counter-ion (Cl, Br, I etc.) rt, 1 – 30 bar H_2	85
Rh NP 2-6 nm	Hydroxyl-functionalized tetraalkyl ammonium w/	Hydrogenation of arenes (biphasic)	360 - 3600 h^{-1} rt, 20 bar H_2	86

	various anions (HTAX) (**8**)			
Rh NP 3 nm	Polyhydroxylated tetraalkyl ammonium chloride (PHTAC) (**10**)	Hydrogenation of arenes (biphasic)	86 - 300 h^{-1} rt, 1 atm H_2	90
Rh NP 2-3 nm	Mono- or tris-hydroxylated tetraalkyl ammonium chloride (HTAC and PHTAC) (**8** and **10**)	Hydrogenation of arenes (biphasic)	75 - 750 h^{-1} rt, 1 atm H_2	122
Ir NP 1.9 nm	Hydroxyl-functionalized tetraalkyl ammonium chloride (HTAC) (**8**)	Hydrogenation of arenes (biphasic)	100 - 400 h^{-1} rt, 1 atm H_2	92
Ru NP 2.5-3.5 nm	Hydroxyl-functionalized tetraalkyl ammonium chloride (HTAC) (**8**)	Hydrogenation of arenes (biphasic)	600 h^{-1}	82
Ru NP 4 nm	Hydroxyl-functionalized tetraalkyl ammonium chloride (**8**) and methylated cyclodextrin (1:1 mixture) (**6c**)	Hydrogenation of arenes (biphasic)	10 - 83 h^{-1} rt, 1 atm H_2	83
Ru NP 1.5 nm	Methylated-α or β or γ-cyclodextrin (Me-CD) (**6c**)	Hydrogenation of arenes (biphasic)	4 - 34 h^{-1} rt, 1 atm H_2	87
Ru NP 2.5 nm	Methylated-α or β or γ-cyclodextrin (Me-CD) (**6c**)	Hydrogenation of arenes (biphasic)	69 h^{-1}	88
Ru NP 2.6 nm	Oleic succinyl β-cyclodextrins (OS-β-CD) (**6d**)	Hydrogenation of arenes (biphasic)	100 % (in 1 – 20 hr) 30 °C, 10 bar H_2 1 mol% Ru	91
Ru NP 1.2-1.5 nm	Alkyl sulfonated diphosphines (**22**)	Hydrogenation of arenes (biphasic)	Up to 100 % rt, 1 or 10 bar H_2	113
Rh NP 1.3 nm Rh NP / GO	Cobaticinium chloride ($[CoCp_2]Cl$) (**3**)	Benzene hydrogenation	12.4 h^{-1} 14.6 h^{-1} (GO)	71

3.3. Reduction of Nitrophenol and Other Nitroaromatics

4-Nitrophenol reduction has been popularly used as a model reaction for the catalytic activity of water-soluble metal nanoparticles (Table 5), because the reaction is generally without any side reactions and can be monitored real-time *in situ* using UV−vis spectroscopy.[99,123] The reaction conversion can be simply determined from the change in intensity of nitrophenolate absorbance at 400 nm that is induced by the reduction of nitro group by $NaBH_4$ or molecular H_2 (Figure 4).

The reaction also could proceed through an electrochemical mechanism involving the electron transfer through the nanoparticle surface from the reducing agent (electron donor) to the substrate (electron acceptor).

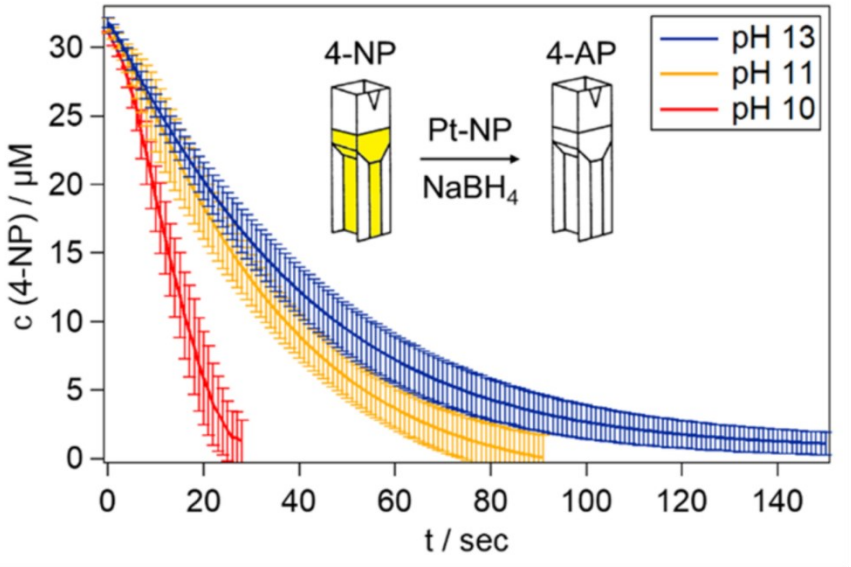

Figure 4. Concentration-time plots of the pH-dependent platinum-catalyzed 4-NP reduction with sodium borohydride as the reducing agent (1000-fold excess), measured by UV/vis absorption spectroscopy (at 400 nm = λ_{max} of 4-NP) [Reproduced with the permission of ref (99). Copyright 2020 American Chemical Society].

4-Nitrophenols and other nitroaromatics are often the ingredients of herbicides and insecticides and known to be common organic pollutants of wastewater.[124] Developing an efficient way to remove nitroaromatics, therefore, has been interests of scientific communities. In addition, the reaction products, aminoaromatics, are considered valuable intermediates for manufacturing chemicals such as analgesics and antipyretics. The mechanistic study by Corma et al. describes both the direct conversion route of 4-nitrophenol to 4-aminophenol and the indirect route involving azo intermediates (Scheme 3).[125]

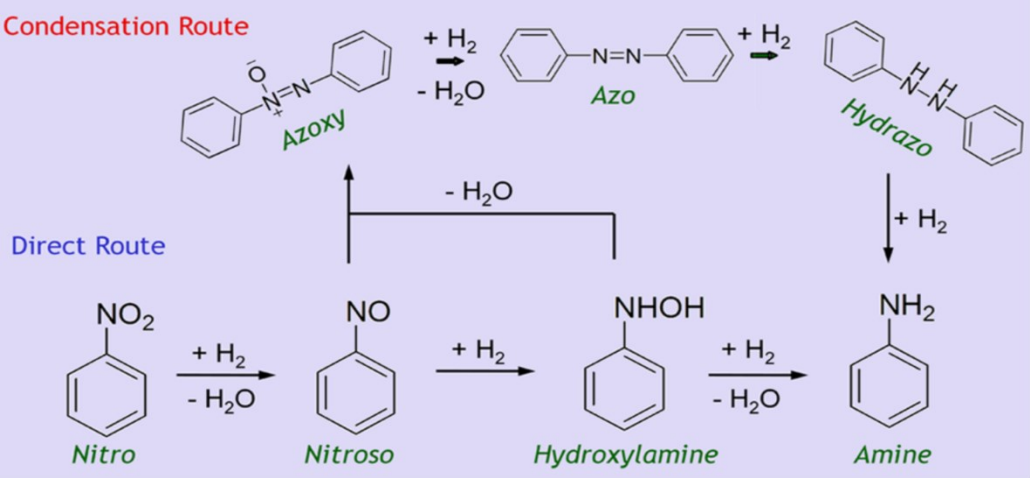

Scheme 3. Reaction route proposed by Haber for the hydrogenation of nitroaromatic compounds. Names below each structure refer to the prefix that identifies the nitrogen functional group [Reproduced with the permission of ref (125). Copyright 2015 American Chemical Society].

3.3.1. In-situ generated or bare metal nanoparticles

Pal and co-workers have first explored the aqueous suspension of silver nanoparticles (AgNPs) as a catalyst to reduce a series of nitroaromatics such as 2-nitrophenol (2-NP), 4-nitrophenol (4-NP), and 4-nitroaniline (4-NA) in the presence of sodium borohydride ($NaBH_4$).[98] The catalysis of *in situ* generated AgNPs was demonstrated using both growing NPs (growing microelectrode-GME) and fully grown NPs (full-grown microelectrode-FGME). In the case of GME, an appropriate amount of $AgNO_3$ was introduced in a proper mixture of water, nitro compounds, and $NaBH_4$. For FGME, the measured amount of $NaBH_4$ was added into prepared fresh AgNP sol (prepared using $NaBH_4$, N_2H_4, CO, or ascorbic acid) before introducing nitro compounds in the mixture. There was no reduction of the nitro aromatic compounds when using only $NaBH_4$ without AgNPs in both cases. Although the conversions of 4-NP, 2-NP, and 4-NA to their corresponding amino products were observed during both GME and FGME processes, the

conversion time or yield of products was not clearly mentioned in the report for all substrates except for 4-NP (73 % conversion). Colorimetric and spectrophotochemical measurements of the reactions have shown that the rate of reduction follows the order of 4-NP > 2-NP > 4-NA.

The role of the pH value on the kinetics of 4-NP reduction by bare AuNPs, PdNPs, and PtNPs was demonstrated in the presence of $NaBH_4$.[99] A slow yet dominant hydride-induced reaction was observed for all three noble-metal catalysts under extreme basic condition (pH ≥ 13). When the pH was lowered from 13 to 10, a faster reduction has occurred for all the catalysts. It was found that dropping the pH from 13 to 10 decreases the half-life time from 28 to 12 s, 18 to 7 s, and 59 to 17s for PtNPs, PdNPs, and AuNPs, respectively. A pseudo-first-order (1, R^2 0.995) reaction kinetics was observed for all catalysts at pH 13 in the presence of excess $NaBH_4$. In contrast, lower reaction order (0.5 and 0) with relatively high regression coefficients was observed at pH 10 for all three catalysts.

3.3.2. Citrate-capped metal nanoparticles

Citrate-stabilized colloidal AuNP ($AuNP_{col}$) catalysts were studied to compare the catalytic activity of colloidal AuNP in a free state with that of TiO_2 supported AuNP ($AuNP_{sup}$) using the reduction of 4-NP in the presence of $NaBH_4$.[65] A gradual increase of rate constants was observed with an increase in the loading of both $AuNP_{col}$ and $AuNP_{sup}$ catalyst, which has suggested the kinetic dependence of the reaction on concentration and available surface area of AuNP. In contrast, a significant decrease of rate constant was observed when $AuNP_{sup}$ catalyst was used instead of $AuNP_{col}$ catalyst. The possible reason for this decrease was the reduction of the surface area of AuNP in the immobilized state (*ca*. 60 % loss of available surface area), change of particle size, restructuring of surface, and synergistic effects, including generation of a unique active site at the AuNP-TiO_2 interfaces and charge transfer between TiO_2 and AuNP.

3.3.3. Alkanethiolate-capped metal nanoparticles

Water-soluble thiolate-protected Au nanocluster, $Au_{25}(SR)_{18}$, was reported to catalyze the reduction of 4-NP in the presence of excess $NaBH_4$ in aqueous solution.[97] This study explored the role of chain length and functional groups of thiolate ligands on catalytic activity as well as the accessibility of the catalysts. Catalytic activity was found to be decreased with the increasing chain length of ligand attached to Au nanoclusters from short, i.e., C3-chain 3-mercaptopropanoic acid (MPA) and C6-chain 6-mercaptohexanoic acid (MHA) to long, i.e., C8-chain 8-mercaptooctanoic acid (MOA) and C11-chain 11-mercaptoundecanoic acid (MUA). The increasing trend of the induction time (26 s for $Au_{25}(MPA)_{18}$ and 326 s for $Au_{25}(MUA)_{18}$), and decreasing trend of the reaction rate constant, k_{app} (0.08 s^{-1} for $Au_{25}(MPA)_{18}$ and 0.007 s^{-1} for $Au_{25}(MUA)_{18}$) indicated a diffusion-controlled reaction kinetics. In contrast, the catalytic activity of $Au_{25}(SR)_{18}$ NCs was not found to be diffusion-controlled by functional groups of the ligands such as MPA (carboxyl group), l-cysteine (l-Cys; one carboxyl and one amine group), and *para*-mercaptobenzoic acid (p-MBA; benzoic acid). In this case, coordination and packing density of the ligands have played more important role on catalytic activity. It was reported that $Au_{25}(p\text{-}MBA)_{18}$ NCs exhibited the lowest induction time (2 s) and the largest K_{app} (0.065 s^{-1}) among all the synthesized catalysts. The π–π stacking effect between the benzene ring on p-MBA and 4-nitrophenol was claimed to facilitate the reactants to penetrate more easily inside the ligand shell and approach the Au active sites. On the other hand, bis-thiolate ligands, MPA/Cys-protected Au nanoclusters were found to give negative catalytic results because of the combined steric hindrance and electronic modifications to the Au core.

3.3.4. Cyclodextrin-capped metal nanoparticles

A stable aqueous dispersion of α-cyclodextrin (α-CD)-capped Au nanoparticles (AuNPs) was reported by Qi, et al. as an effective catalyst for the reduction of 4-NP into 4-AP in the presence of $NaBH_4$.[74] The conversion revealed that 80 to 90% of 4-NP was reduced in 10 min in the presence of AuNPs with different core sizes (11, 20, and 26 nm) with the pseudo-first-order nature.

3.3.5. Other ligand-capped metal nanoparticles

Anionic water-soluble leaning pillar[6]arenes (AWLP6)-stabilized AuNPs (AWLP6-AuNP) studied by Yang was found to be an efficient catalyst for the complete conversion of 4-NP to 4-AP within 30 min and with the measured rate constant of 0.156 min^{-1}.[73] The AWLP6-mediated stability and larger particle size (average diameter 11.1 ± 1.7 nm) of AuNP were reported to provide more appropriate specific surface areas for the adsorption of 4-NP molecules. The flexible skeleton structures of AWLP6 seems to benefit the stable adsorption of the ligand on AuNP surface and attaining suitable catalytic environments by slightly adjusting the conformations. Reduction of 4-NP to 4-AP was also observed by tannic acid-capped colloidal AuNP (TA-AuNPs) with different concentrations of tannic acid.[70] It was revealed that a complete conversion of 4-NP takes two times longer (2,800 vs 1,440 sec) by TA-AuNPs prepared in higher concentration of TA (0.3 mM vs 0.2 mM). Addition of graphene oxide to TA-AuNPs was found to increase the reaction rate further (720 sec with 0.3 mM TA and 360 sec with 0.2 mM Ta). A pseudo first order reaction kinetics was calculated in all cases.

Other noble metal nanoparticles have shown activities for the reduction of 4-NP to 4-AP. The reduction of 4-NP in water was demonstrated using amphiphilic viologen (1,10-dioctadecyl-4,40-bipyridinium bromide, $C_{18}V^{2+}$)-stabilized platinum NPs (PtNPs–viologen micelles).[117] Approximately 90% reduction was observed within 15 min in the presence of PtNPs–viologen

micelles. In contrast, the aggregation of surfactant-free PtNPs has caused a decrease in surface area and ultimately lowered the catalytic activity by hindering the diffusion of 4-NP molecules through the NPs surface. However, well dispersed and evenly distributed PtNP in viologen micelles has offered an increase in the surface area and led to a higher catalytic activity. A reduction of 4-NP to 4-AP using aqueous dispersed cobalticinium chloride-stabilized RhNPs and graphene oxide-RhNPs (GO/RhNPs) hybrids was demonstrated in the presence of excess $NaBH_4$ at 20 °C.[71] An efficient and complete conversion was reported by both catalysts with the rate constants of 0.0158 and 0.0163 s^{-1} for cobalticinium chloride-stabilized RhNPs and GO/RhNPs, respectively.

Table 5. Reduction of Nitrophenols and Nitroaromatics Catalyzed by Novel Metal Nanoparticles in Water under Single Phasic.

Catalysts	Ligand Stabilizers	Catalytic Reactions	Catalysis Notes	References
Ag NP	Bare – likely Borohydride (**15**)	Reduction of nitroaromatics (4-nitrophenol, etc.)	>73-95%	98
Pd, Pt, and Au NP 3-5 nm	Bare – likely Borohydride (**15**)	Reduction of 4-nitrophenol	pH = 13 and 10 : faster at lower pH hydride-driven reaction	99
Au NP 5.6 nm	Citrate (**1**)	Reduction of 4-nitrophenol	Up to 2.2 min^{-1} Colloidal vs supported	65
Au NC 1 nm – Au_{25}	Hydrophilic alkane- and arene-thiols (**13**)	Reduction of 4-nitrophenol	Up to 4.8 min^{-1}	97
Au NP 10-50 nm	α-Cyclodextrin (**6a**)	Reduction of 4-nitrophenol	0.28 min^{-1}	74
Au NP 11 nm	Anionic water-soluble leaning pillar[6]arene (AWLP6) (**5**)	Reduction of 4-nitrophenol	0.156 min^{-1}	73
Au NP 18-35 nm Au NP/GO	Tannic acid (**2**)	Reduction of 4-nitrophenol	0.21 min^{-1} 0.47 min^{-1}	70

12-33 nm				
Pt NP 1 nm	Octadecyl viologen micelles (**24**)	Reduction of 4-nitrophenol	>95 % in 15 min	117
Rh NP 1.3 nm Rh NP / GO	Cobaticinium chloride ([$CoCp_2$]Cl) (**3**)	Reduction of 4-nitrophenol	0.95 min^{-1} 0.98 min^{-1} (GO)	71

3.4. Carbon-Carbon Cross Coupling and Homocoupling Reactions

Carbon-carbon coupling reactions such as Heck, Suzuki, Negishi, Stille, Sonogashira, and Buchwald-Hartwig reactions are considered as the most versatile tools for organic synthesis in both academics and industries.[126] All these reactions catalyzed by transition metal complexes have seen tremendous success and popularity with developments in their ligand chemistry that resulted in the necessary activity enhancement with synthetically useful rate. Among various metal centers that in principle capable of catalyzing these reactions, Pd clearly dominated the synthetic applications in laboratories and industries related to the production of polymers, pharmaceutical intermediates, agricultural chemicals, and new technological materials. This is due to the tolerance of Pd to a wide variety of functional groups.

Nanoscale metal nanoparticles have also gained considerable interests in recent years for their applications as catalysts for carbon-carbon coupling reactions attributable to the simplified separation and recycling processes involving, for example, centrifugation/decantation or (membrane) filtration.[127-129] The availability of Pd nanocatalysts with comparable activities to homogeneous Pd complexes offers an alternative approach for the reactions while avoiding the problems associated with purification and toxic waste production, which are significant concerns in large scale synthetic processes. In addition, the developments in the synthetic protocols for water-soluble Pd nanocatalysts along with the significant benefits of catalysis applications in aqueous media allowed the investigations for water-soluble Pd nanoparticle catalysts on carbon-carbon coupling reactions to pick up the streams recently (Table 6).

In addition to the cross-coupling reactions, the carbon-carbon bond forming homocouplings of organoboron or organohalide compounds were successfully catalyzed by various metal catalysts.[130,131] This reaction has been especially useful for the synthesis of symmetrical functional materials and has also become one of the standard methods to evaluate the reactivity of metal nanoparticles as potential catalysts. Although it is very limited, the example of water-soluble metal nanoparticles used for the C-C homocoupling reaction is also presented.

3.4.1. Tetraalkylammonium ions-capped metal nanoparticles

An aqueous Heck reaction catalyzed by in-situ formed PdNPs stabilized by tetrabutylammonium bromide (TBAB) in water was reported by Zhou et al.[78] The Heck reaction of iodobenzene was carried out with methyl acrylate in the presence of $PdCl_2$, Na_2CO_3, and TBAB in water at 25 °C for 4.5 h with and without ultrasonic irradiation. An enhancement of the yield from 10 to 86 % of the product, (E)-methyl cinnamate, was observed after introducing ultrasonic irradiation. Several aryl iodides and olefins were also investigated under the same ultrasonic aqueous condition. The coupling reactions of iodobenzene with ethyl acrylate, acrylic acid, acrylonitrile, and styrene were found to produce mostly E isomers in the range of 75 to 82 %. The chemoselectivity over 90 % was observed for iodo group when 1-chloro-4-iodobenzene or 1-bromo-4-iodobenzene was employed. However, *ortho*-substituted iodobenzene was not efficient in reacting with olefins smoothly under this condition indicating the steric problem. This report also demonstrated a regioselectivity of *para*- over *ortho*-substitution in several aromatic polyiodides.

In-situ prepared TBAB-stabilized PdNPs in water could catalyze a stereoselective coupling reaction of vicinal-diiodo-(E)-alkenes with acrylic esters and nitriles (Scheme 4 (a)).[76] In-situ PdNPs were found to produce 82% (E)-isomers from acrylic esters exclusively, whereas

(Z)-isomers are obtained in high stereoselectivity from reactions of acrylonitrile. However, relatively lower yield (30 - 40 %) was observed when diiodoalkenes are replaced by dibromoalkenes. Another in-situ generated PdNPs without conventional ligand in water showed one-pot Suzuki coupling of aryl bromides/iodides with aryl- and alkyl boronic acids producing a variety of functionalized biaryls and alkyl-aryls (Scheme 4 (b)).[108] Sodium dodecylsulfate (SDS) was likely acting as a stabilizing ligand for the PdNPs. Most reactions were found to be completed in 5 min with yields higher than 90%. In comparison, the product yields were low in the range of 30 - 50% when organic solvents such as DMF, toluene, and THF are used in place of water. Neither electron-withdrawing nor electron-donating substituent groups on the aromatic ring of aryl halides were reported to affect the reactivity and product yields.

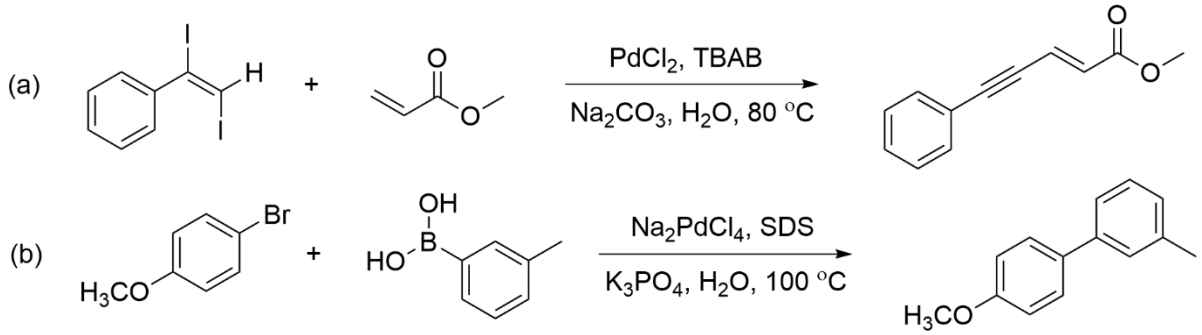

Scheme 4. Representative C-C coupling reactions by *in situ*-generated Pd nanoparticles in water: (a) Reaction of *vic*-diiodoalkenes with an activated alkene[76] and (b) Suzuki coupling reaction.[108]

In situ-generated PdNPs stabilized with a water–soluble ammonium ligand, 1-[*N,N',N''*-trimethyl-(4-butyl)ammonium]-2-(2-pyridyl) imidazole chloride were demonstrated to catalyze Suzuki-Miyaura reaction of aryl chlorides and aryl bromides in air and water.[107] Aryl bromides bearing electron-withdrawing groups, such as MeCO, CN, and NO_2, have yielded 100 % coupling product but a moderate yield (below 80%) was observed for aryl bromides with

electron-donating groups, such as MeO and Me. The steric effect was observed from the sluggish coupling reactions of 2-bromotoluene or 3-bromopyridine (< 90 %). In contrast, cross-coupling reactions of 4- bromoacetophenone with other activated and deactivated aryl boronic acids have yielded 100% biaryl products. In this case, ortho-, meta- and para-substituents in the aromatic ring of boronic acids was not found to affect the reactions. Similarly, water-soluble N,N-dimethyl-N-alkyl-N-(2-hydroxyethyl)ammonium halide salts (HEAnX, n = 16 or 18, X = Cl or Br)-capped PdNPs were investigated for a biphasic catalytic Suzuki reactions under mild conditions.[94] The best result (100 % yield in 30 min) was obtained when HEA16Cl with an R (R= HEAnX/Pd) of 25 was applied for the catalytic reaction of bromobenzene at 60 ºC. The colloidal suspension was found to be stable irrespective of the molar ratio R.

3.4.2. Cyclodextrin-capped metal nanoparticles

2-Hydroxypropyl-α-cyclodextrin (α-HPCD)-capped PdNPs (α-HPCD/PdNP) was reported to catalyze various C-C cross-coupling reactions including Suzuki, Heck, and Sonogashira reactions in water.[75] Aqueous Heck coupling of aryl iodide and styrene using a lower dose of α-HPCD (0.02 mol%) has resulted in 96 % yield (960 h^{-1}) with 100 % selectivity. Poorly soluble aryl halides, however, required higher loading of catalyst (0.1 mol%) for over 90% yield. The same catalyst with higher loading (0.5 mol%) was used to catalyze Sonogashira reactions involving aryl halides and terminal acetylenes to produce moderate to good yield (up to 93 % with a TOF of 186 h^{-1}) in absence of any added typical copper cocatalyst. Suzuki–Miyaura cross-coupling of aryl- or heteroarylboronic acids and halide derivatives took place in the presence of lower dose (0.01 mol%) of α-HPCD/PdNP producing close to 100 % yield with a TON of 10,000. Aqueous perthiolated β-cyclodextrin-capped Pd nanoparticles (β-CD/Pd) were found to catalyze Sonogashira reaction between terminal alkynes (e.g. phenylacetylene) and aryl iodides

(e.g. iodobenzene) in water.[116] The yield of 90 % could be achieved even without additional stabilizing agent (PPh_3) and co-catalyst (CuI) at room temperature.

3.4.3. Other examples

Oleate-capped PdNPs dispersed in aqueous phase could catalyze Suzuki coupling reaction.[105] It was observed that bromobenzene could be coupled with benzene boronic acid to produce biphenyl in up to 99 %. Monopoli et al. have demonstrated that Ullmann-type homocoupling of haloarene could be catalyzed by in-situ generated PdNPs in water at temperatures ranging from 40 to 90 °C.[72] Under optimized conditions calculated amount of bromo- or chloroarenes, glucose or HCOONa as reducing agent, TBAOH (base), and Pd acetate were mixed in water and heated under stirring for 6 h (Scheme 5). Results indicated that conversions of the chloroarene were increased with temperature. Bromoarenes, such as bromobenzene, 4-bromotoluene, 4-bromoanisole, and 3-bromothiophene, were also reported to be coupled in excellent yields in the range of 82-86 % even at low temperature (40° C).

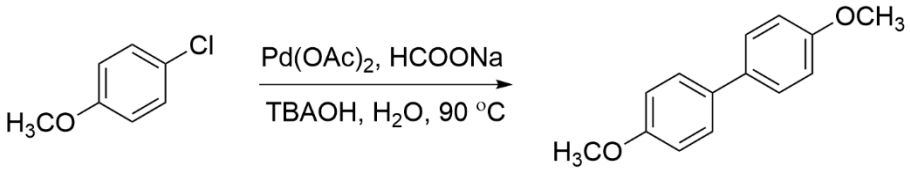

Scheme 5. Reductive homocoupling of 4-chloroanisole using *in situ*-generated Pd nanoparticles in water.[72]

Table 6. Carbon-Carbon Cross-Coupling and Homocoupling Reactions Catalyzed by Novel Metal Nanoparticles in Water.

Catalysts	Ligand Stabilizers	Catalytic Reactions	Catalysis Notes	References
Pd NP	Tetrabutylammonium bromide (TBAB) (**7**)	Heck coupling (in situ)	Up to 93% (1 mol% Pd) Ultrasonic irradiation promote the rate	78

			of reaction	
Pd NP 2-6 nm	Tetrabutylammonium bromide (TBAB) (**7**)	Tandem Heck coupling-elimination to form enynes (in situ)	82% (100 E selectivity)	76
Pd NP 6-8 nm	Sodium dodecylsulfate (SDS) (**19**)	Suzuki coupling (in situ)	90 - 96% (5 min rxns)	108
Pd NP 3 nm	Pyrydyl imidazole-functionalized tetraalkylammonium chloride (**18**)	Suzuki-Miyaura coupling (in situ)	100% (0.1 mol% Pd) Effect of substituents	107
Pd NP Size – N.A.	Hydroxyl-functionalized tetraalkyl ammonium chloride (HTAC) (**8**)	Suzuki coupling (biphasic)	100% (1 mol% Pd)	94
Pd NP 2-7 nm	Hydroxypropyl-α-cyclodextrin (HP-CD) (**6b**)	Heck Suzuki-Miyaura Sonogashira	96% (960 h^{-1}) 100% 93% (186 h^{-1})	75
Pd NP 3 nm	Thiolated-β- cyclodextrin (**23**)	Sonogashira coupling	90 % (10 mol% Pd)	116
Pd NP 3.8 nm	Oleate (**17b**)	Suzuki coupling	Up to 99 % (0.3 mol% Pd)	105
Pd NP 15 nm	Glucose (**4**)	Homocoupling of arylhalides	73-95 %	72

3.5. Other Miscellaneous Catalytic Reactions

There are several other reactions that were found to be catalyzed by water-soluble noble metal nanoparticles in water or water-organic biphasic conditions beside the hydrogenations, C-C coupling reactions, and nitroaromatic reductions (Table 7).

3.5.1. Carbonyl reduction

Jin et al. have shown that a series of water-soluble $Au_n(SR)_m$ nanoclusters including glutathione-capped $Au_{15}(SG)_{13}$, $Au_{18}(SG)_{14}$, $Au_{25}(SG)_{18}$, $Au_{38}(SG)_{24}$, and captopril-capped $Au_{25}(Capt)_{18}$ could catalyze the chemoselective hydrogenation of 4-nitrobenzaldehyde (4-NO_2PhCHO) to 4-nitrobenzyl alcohol (4-NO_2PhCH_2OH) with ~100% selectivity in aqueous media under relatively mild conditions.[118] The effects of the Au core (from Au_{15} to Au_{38}, size range from ~0.8 to ~1.3

nm) on the conversion rate have hinted the size and ligand-dependent catalytic activity. It was demonstrated that $Au_{15}(SG)_{13}$ was only capable of converting 7.8% of 4-nitrobenzaldehyde, whereas the increase of core size to $Au_{18}(SG)_{14}$, $Au_{25}(SG)_{18}$, and $Au_{38}(SG)_{24}$ resulted in the increase of yields to 10.2, 16.0, and 20.6 %, respectively (Figure 5). Under similar reaction conditions, an improved conversion rate (23.3 %) was observed by captopril mediated cluster, $Au_{25}(capt)_{18}$. It was proposed that the less bulkiness of captopril over glutathione might have played an important role behind the catalytic efficiency.

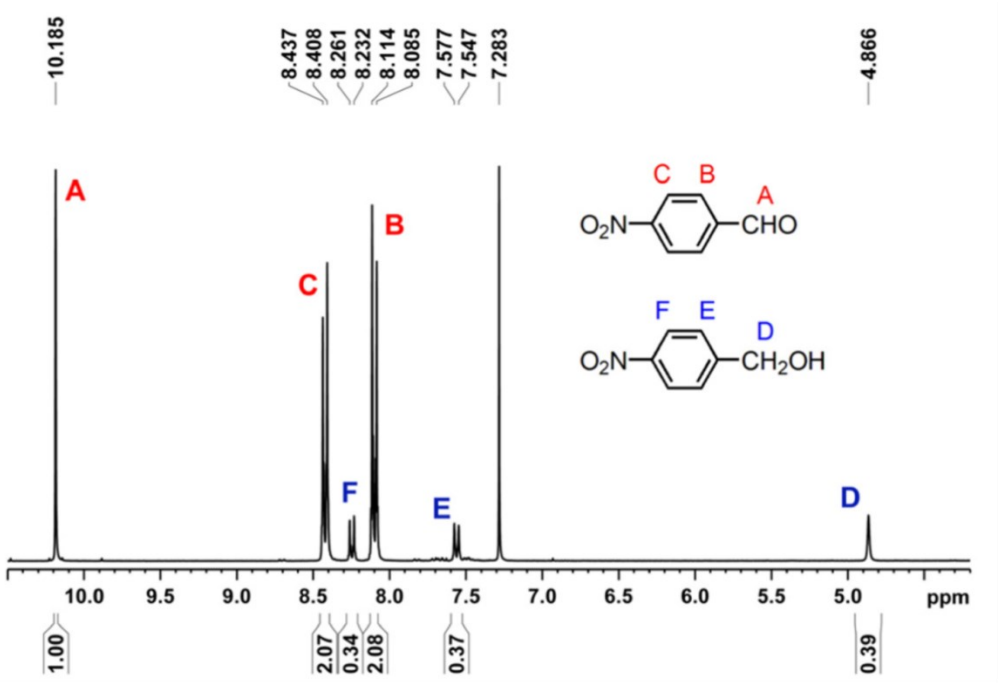

Figure 5. ^{1}H NMR spectrum of the crude product after the catalytic reaction catalyzed by the $Au_{25}(SG)_{18}$ nanocluster catalyst. Only residual reactant 4-nitrobenzaldehyde (-C***H***O at 10.18 (A), the proton on the phenyl ring at 8.44 and 8.41 (C), 8.11 and 8.08 (B) ppm) and the exclusive 4-nitrobenzyl alcohol product (-C$\boldsymbol{H}_2$ at 4.87 (D), the proton on phenyl ring at 8.26 and 8.23 (F), 7.58, and 7.55 (E) ppm) are found in the spectrum [Reproduced with the permission of ref (118). Copyright 2014 American Chemical Society].

AuNPs and Au nanorods were found to be efficient for the chemoselective conversion of 4-nitrobenzaldehyde to 4-nitrobenzyl alcohol with 100 % selectivity in water with a trace amount of pyridine.[64] Pyridine has played an important role as a promoter during the reaction as no reaction was initiated even after the use of an excessive amount of Au nanostructures. The conversion rate was found to be affected by temperature during the use of citrate-capped AuNPs with yields of 15, 33, and 53 % at 25, 55 and 80 ^{o}C, respectively. However, AuNPs started to aggregate and precipitated out at 80 ^{o}C because of inherently insufficient thermal stability of the particles. In contrast, cetyltrimethylammonium bromide (CTAB)-protected Au nanospheres and nanorods of four different lengths and widths have exhibited better thermal stability and catalytic activity under similar reaction conditions. It was found that all four types of nanorods have converted >99% of 4-nitrobenzaldehyde to 4-nitrobenzyl alcohol with 100% selectivity, whereas 27 % of conversion with 100% selectivity was observed for CTAB-capped nanospheres.

The alkyl sulfonated diphosphine-stabilized RuNPs were active for hydrogenation of acetophenone at both atmospheric and high pressure reaction conditions.[113] Hydrogenation of acetophenone has led to the formation of phenylethan-1-ol (84 %) and cyclohexylethan-1-ol (15 %) after 20 hr of reaction at atmospheric condition. Under 10 bar of H_2, however, a total conversion of acetophenone to the cyclohexylethan-1-ol had taken place. Oleic succinyl β-cyclodextrin-stabilized RuNPs ((Ru_OS-β-CD NPs) could catalyze the aqueous hydrogenation of aromatic carbonyl compounds under a hydrogen pressure of 10 bar at room temperature.[91] For instance, benzaldehyde was completely converted into benzyl alcohol in the first phase of reaction which was followed by the reduction of the aromatic ring. The complete conversion to its fully saturated equivalent required 1,140 minutes. The hydrogenation of furfural was also reported to convert the aromatic carbonyl to the saturated alcohol after 840 mins.

In situ-generated RuNP formed by the reduction of various Ru–N-heterocyclic carbene (NHC) complexes using dihydrogen could catalyze the hydrogenation of ester group in levulinic acid and the subsequent lactonization to γ-valerolactone in water.[101] The most successful catalytic transformation of levulinic acid to γ-valerolactone with a conversion of >99% was achieved by RuNP generated from [$RuCl_2$(p-cymene)($^iPr_2$-imy)] (imy: imidazole; TON of 963 and TOF of 361 h^{-1}) and [$RuCl_2$(p-cymene) ($^iPr_2$-bimy)] (bimy: benzimidazole; TON of 999 and TOF of 374 h^{-1}) in aqueous media among the other tested solvents including methanol, IPA, THF, and 1,4-Dioxane. The observation of reaction kinetics revealed that the overall reaction was zero order across the catalysts.

Water soluble PtNPs and RhNPs have exhibited an activity for catalytic enantioselective hydrogenation of ethyl pyruvate in biphasic and aqueous conditions.[89,102] PtNPs were stabilized by HEA16Cl, N,N-dimethyl-N-cetyl-N-(2-hydroxyethyl)ammonium chloride salt, and modified with (−)-cinchonidine.[102] RhNPs were protected with NMeEph12X, the water-soluble family of optically active N-methylephedrium salts containing various counter-ions (X = Br, HCO_3, or (S)-lactate) and a dodecyl alkyl chain (Scheme 6).[89] Enantioselective hydrogenations conducted by PtNPs under various reaction conditions indicated that optimal enantioselective excess (e.e.) value of 48% was obtained at S/Pt = 400 after 30 min of reaction under 20 bar H_2 (Figure 6). A significant difference in e.e. was observed during an increase of hydrogen pressure from 1 (e.e. = 32%) to 20 bar (e.e. = 49%). In contrast, only 55% e.e. was achieved even after elevating the pressure up to 40 bar. However, in terms of reaction time, 55% e.e. was the best-reported result as it took only 13 min at 40 bar of pressure. The catalytic activity and enantioselectivity of RhNP catalytic system for the hydrogenation of ethylpyruvate was also affected by hydrogen pressure. The successful conversion occurred when the reactions are under >20 bar of H_2 (83 % in 7 hr).

The optimal condition was 40 bar of H_2 leading to a complete conversion in 1 h with 12% e.e. The stereoselectivity could increase with the use of (-)-cinchonidine (15% e.e.) and the combination of (S)-(-)-lactate and (-) cinchonidine (18 % e.e.) as additives.

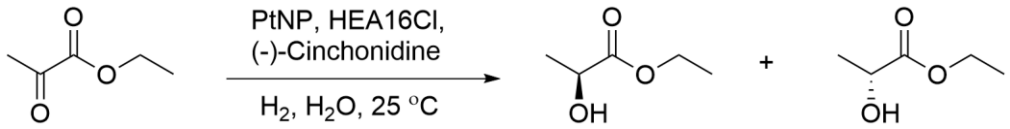

Scheme 6. Asymmetric hydrogenation of ethylpyruvate with PtNPs stabilized by HEA16Cl.[102]

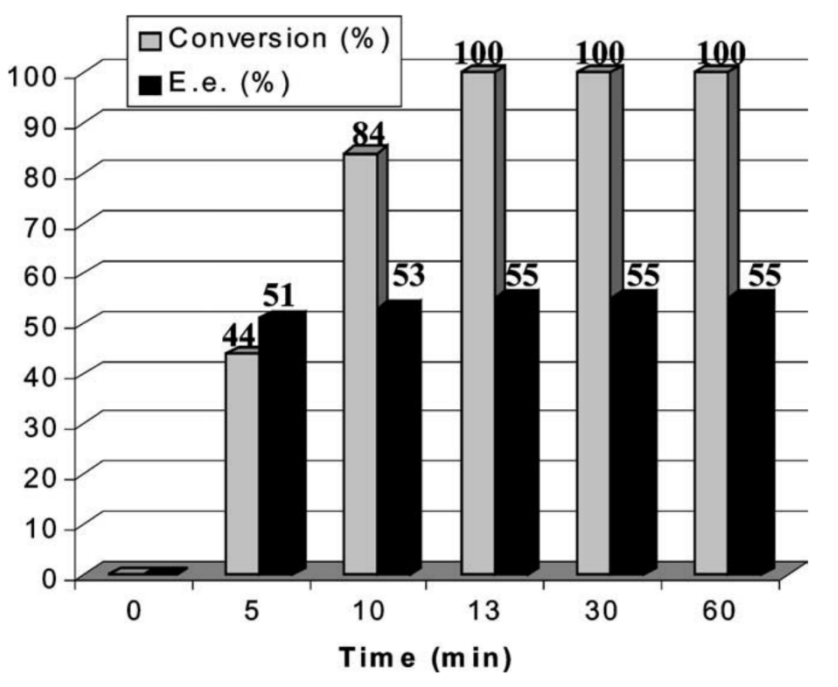

Figure 6. Effect of ethyl pyruvate conversion on enantiomeric excess values [Reproduced with the permission of ref (102). Copyright 2004 Elsevier].

3.5.2. Dehalogenation of haloarenes

The dehalogenation of various haloarenes using PdNPs stabilized by HEA16Cl (Pd/HEA16Cl) was demonstrated.[93] Chlorobenzene was completely converted to benzene in about 3 and 1.5 hr

at atmospheric hydrogen pressure and 10 bar of pressure, respectively. In contrast, the reactions took almost 24 hr for the dehalogenation of 2-chlorophenol, 4-chloroanisole, and 4-chlorotoluene into benzene derivatives under the same reaction conditions. The results indicated the kinetics of the reactions were not greatly influenced by the pressure of hydrogen but the nature of the functional groups. Bromobenzene could also be completely dehalogenated to benzene after longer reaction times of 3.2 and 10.3 hr. However, the dehalogenation of iodobenzene was not observed even after the extended reaction time. These results have implied that the cleavage of the C-I bond is much more challenging than those of C–Br bond (281 $kJ \cdot mol^{-1}$) and the C–Cl bond (340.2 $kJ \cdot mol^{-1}$). The hydrodechlorination of chlorobenzene and chlorotoluene has also been performed by the aqueous suspension of RhNP at the pressure of 10 bar.[84] It was found that RhNP was successful not only towards the cleavage of the C–Cl bond but also to the complete hydrogenation of the aromatic ring, whereas the Pd/HEA16Cl system was only limited to the hydrogenolysis of the C–Cl bond.

Water-soluble oleate-stabilized PdNP was reported for the dehalogenation reaction of aryl chloride in water. The results indicated that PdNP (0.8 mol% relative to substrate) has successfully converted aryl halide to yield a product in 98 % after 3 hr of reaction.[105] However, a reduced activity was observed in the second and third trials due to the removal of the capping ligands during the catalytic process.

3.5.3. Hydrolysis of ammoniaborane

Water-soluble laurate (dodecanoate)-stabilized RhNPs and RuNPs were reported to be active for the hydrolysis of ammoniaborane (AB) which results in hydrogen generation.[103,104] A complete release of H_2 (3.0 mol H_2/mol AB) was recorded by both catalysts within 6 and 8 min,

respectively. The corresponding TOF value was calculated as 200 and 75 min^{-1} by RhNP and RuNP, respectively, at 25.0 °C. Water-soluble cobalticinium chloride-stabilized RhNP catalysts and supported RhNPs on rGO (RhNP/rGO) were also reported to catalyze the hydrolysis of ammonia borane in aqueous media.[71] The complete hydrolysis of AB was achieved in 8.5 min with a corresponding TOF value of 14,286 h^{-1}, whereas a TOF value of 22,222 h^{-1} was recorded in the presence of RhNP/rGO.

3.5.4. Hydrgenolysis of epoxides

The efficient hydrogenolysis of benzylic epoxides was demonstrated by water-soluble PdNP stabilized with tetrabutylammonium bromide.[106] The catalysis results indicated that, in comparison to other organic solvents such as methanol, ethyl acetate, and acetonitrile, water is the best medium. A complete conversion of styrene oxide to the corresponding alcohol (97%) was observed by PdNPs (Pd/substrate = 1%) in 20 hr at room temperature and under a hydrogen atmosphere in water. Chemoselective hydrogenolysis of epoxides in water was observed from the hydrogenolysis of 2-(4-chlorophenyl)oxirane, 2-(3-chlorophenyl)oxirane, and benzyl 3-phenyloxirane-2-carboxylate, which took place without reduction of reactive functional groups including chloro and carboxylate groups.

3.5.5. C-H activation reactions

Catalytic properties of two water-soluble RuNPs (Ru@**1** and Ru@**2**) stabilized by sulfonated N-heterocyclic carbene (NHC) ligands (1-(2,6-diisopropylphenyl)-3-(3-potassium sulfonatopropyl)imidazol-2-ylidene (**A**) and 1-(2,4,6-trimethylphenyl)-3-(3-potassium sulfonatopropyl)-imidazol-2-ylidene (**B**)) were reported towards the deuteration of L-lysine in water through C–H activation.[100] An insignificant (reduced or zero) exchange of C-H/D was

observed at α (0 – 29 %), β, γ, δ, and ε (0 - 12%) position of L-lysine for Ru@**A** at lower pH (1.6 - 3.2). With enhanced catalytic activity at the pH > 6.9, the best results were achieved from the C-H activation reactions in the range of pH 10.4 to 13.2, where H/D conversion was calculated as high as 99 and 98.5 % at α and ε position, respectively (Figure 7).

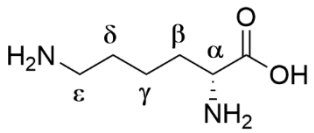

Figure 7. Structure of L-lysine.

The selective H–D exchange at carbons α to the endocyclic N atom of the aromatic ring of pyridine-containing compounds in D_2O was demonstrated by water-soluble PdNP.[95] The effects of temperature (RT, 50 °C and 80 °C) and dispersion age of nanoparticles (fresh and 1-month-old) were investigated. The rapid exchange of α proton along with ~16 % of the β protons at elevated temperature (5 h at 80 °C) indicated the acceleration of reaction rate with increased temperature but the compromise in the selectivity was clearly presented. In comparison, no β-proton exchange was observed at room temperature. The faster H–D exchange rate was reported from the fresh dispersion than the aged dispersion because of the formation of Pd–O surface species.

Tetrabutyl ammonium bromide (TBAB)-stabilized PdNPs could catalyze Knoevenagel condensation, Michael addition, and tautomerization reaction, which involve C-H activation reaction as their key steps.[77] Coumarine, indole, dimedone and pyrazolone were used as substrates to react with aryl aldehyde in the presence of PdNPs to produce different derivatives of bis(heterocyclyl)methane. Water was found to be the best solvent producing the products in

higher yields (86-92%) within 0.3-1.5 hr over other solvents including acetonitrile, dichloromethane, and tetrahydrofuran (THF).

3.5.6. Dye decomposition reactions

Water-soluble and highly monodisperse sodium citrate (SC) and tannic acid (TA)-coated spherical silver nanoparticles (AgNPs) was reported for the reduction of Rhodamine B (RhB) in the presence of sodium borohydride.[63] RhB was degraded in 30 min by SC/TA-stabilized AgNPs (Figure 8). For comparison, the activity of PVP-coated AgNP was compared but the incomplete reduction was observed. Since PVP, a long bulky polymer, can inhibit the diffusion of RhB molecules toward the catalytic Ag-core, this observation hinted that the catalytic activity of the AgNPs was influenced by the composition of the organic shell and the surfactant used in the synthetic process.

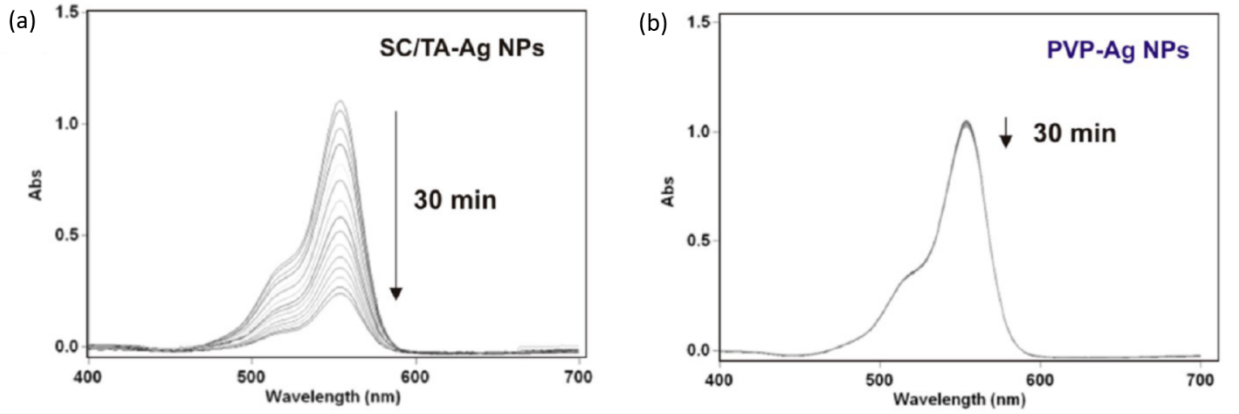

Figure 8. Catalytic properties of as-synthesized SC/TA-stabilized Ag NPs and PVP-coated Ag NPs. Decrease in Rhodamine B concentration over time using SC/TA-stabilized Ag NPs (A) and PVP-coated Ag NPs (B) catalysts [Reproduced with the permission of ref (63). Copyright 2014 American Chemical Society].

Colloidal core-shell Ag@Pd NPs was reported for the successful degradation of Congo Red, Direct Blue 14, and Sunset Yellow dyes.[68] The degradation rate was found to be affected by the structure of the dye. The electron-donating group causes the increase of electron density around the chromophores' structure (–N=N–), which facilitates the degradation of dyes by breaking the azo bond. The reaction rate of Direct blue, which contain more (six) electron-donating group (OH, -NH_2, -CH_2) than withdrawing groups (-SO_3Na), was higher (0.1319 mol·$l^{-1}$$min^{-1}$) than that of Congo red (contains the equal number of donating and withdrawing groups) (0.1059 mol·$l^{-1}$$min^{-1}$) and Sunset yellow (only one donating group and two withdrawing group) (0.0299 mol·$l^{-1}$$min^{-1}$) with the degradation of 95, 90 and 84 %, respectively. Water soluble 4-sulfocalix[4] arene (SC)-stabilized RuNPs (Ru@SC) was studied as an efficient catalyst for the reduction of toxic brilliant yellow (BY) into amine product in the presence of $N_2H_2 \cdot H_2O$.[96] The reduction kinetics of the reaction has revealed the rate constant of 0.212 min^{-1}, which was calculated and claimed as 8.83, 11.8, and 8.15 times higher than the commercial Ru/C (5 %) (ruthenium 5 % on activated charcoal), Pd/C (5 %), and Pd/C (10 %), respectively. Besides the synthetic sample, real sample like contaminated river water was explored and a competitive rate constant of 0.165 min^{-1} was achieved by this catalytic system.

Table 7. Other Miscellaneous Reactions Catalyzed by Novel Metal Nanoparticles in Water.

Catalysts	Ligand Stabilizers	Catalytic Reactions	Catalysis Notes	References
Au NC 1-1.5 nm $Au_n(SR)_m$	Glutathione (**25a**) Captopril (**25b**)	Chemoselective hydrogenation of 4-nitrobenzaldehyde to 4-nitrobenzyl alcohol (biphasic)	30 h^{-1} (23%) - 100% selectivity 80°C, 20 bar H_2	118
Au NP 18 nm	Citrate (**1**)	Hydrogenation of 4-	>99% yield - 100%	64

Au nanorods ~20 nm + ~40 nm (width + length)	Cetyltrimethyl-ammonium bromide (CTAB) (**14**)	nitrobenzaldehyde to 4-nitrobenzyl alcohol (biphasic)	selectivity 80°C, 20 bar H_2	
Ru NP 1.2-1.5 nm	Alkyl sulfonated diphosphines (**22**)	Hydrogenation of ketone in biphasic condition	Up to 100 %	113
Ru NP 2.6 nm	Oleic succinyl β-cyclodextrins (OS-β-CD) (**6d**)	Hydrogenation of carbonyls	100 % hydrogenation in 60 – 3800 min using 1 mol% Ru	91
Ru NP 4 nm	Imidazolium N-heterocyclic carbene (NHC) (**16**)	Hydrogenation of ester (levulinic acid to valerolactone)	361 h^{-1}	101
Pt NP 2.5 nm	Hydroxyl-functionalized tetraalkyl ammonium chloride (HTAC) (**8**)	Asymmetric hydrogenation of ethylpyruvate	100% (55% ee) 1-40 bar H_2	102
Rh NP 2.5 nm	N-Methylephedrium salts (**9**)	Asymmetric hydrogenation of ethylpyruvate	100% (18% ee) 20 bar H_2	89
Pd NP 2.7 nm	Hydroxyl-functionalized tetraalkyl ammonium chloride (HTAC) (**8**)	Dehalogenation of halogenoarenes to arenes	10 h^{-1} 100% (1 mol% Pd) 20°C, 1-10 bar H_2	93
Rh NP 2.7 nm	Hydroxyl-functionalized tetraalkyl ammonium chloride (HTAC) (**8**)	Tandem dehalogenation and hydrogenation of halogenoarenes	220 h^{-1} 10 bar H_2	84
Pd NP 3.8 nm	Oleate (**17b**)	De-chlorination of aryl chloride	>98 % (0.8 mol% Pd)	105
Rh NP 5.2 nm	Laurate (**17a**)	Hydrolysis of ammonia-borane	200 min^{-1} (0.25 mol% Rh), 25°C	104
Ru NP 2.6 nm	Laurate (**17a**)	Hydrolysis of ammonia-borane	75 min^{-1} (0.50 mol% Ru), 25°C	103
Rh NP 1.3 nm Rh NP / GO	Cobaticinium chloride ([$CoCp_2$]Cl) (**3**)	Ammonia borane hydrolysis Transfer hydrogenation	14290 h^{-1} 22222 h^{-1} (GO) 2.0 h^{-1} 3.9 h^{-1} (GO)	71
Pd NP	Tetrabutylammonium	In situ chemo- and	97%	106

Size – N.A.	bromide (TBAB) (**7**)	region-selective hydrolysis of epoxides > ester, aryl halide in water		
Ru NP 1.5 nm	Sulfonated N-heterocyclic carbene (NHC) (**16**)	C-H deuteration of L-lysine	99%	100
Pd NP 3.4 nm	4-Dimethylamino-pyridine (DMAP) (**11**)	C-H deuteration of pyridine based molecules	<90% exchange	95
Pd NP 20-50 nm	Tetrabutylammonium bromide (TBAB) (**7**)	Tandem Knoevenagel condensation followed by Michael addition	92%	77
Ag NP 10-200 nm	Citrate (**1**) Tannic acid (**2**)	Reduction of Rhodamine B	0.064 min^{-1}	63
Ag@Pd NP 10 nm	Citrate (**1**)	Dye degradation (Congo red, Direct blue 14, Sunset yellow)	0.1059 $molL^{-1}min^{-1}$ 0.1318 $molL^{-1}min^{-1}$ 0.0299 $molL^{-1}min^{-1}$	68
Ru NP 5 nm	4-Sulfocarlix[4]arenes (**12**)	Reduction of brilliant yellow azo dye	0.212 min^{-1}	96

CONCLUSIONS AND FUTURE DIRECTIONS

Water-soluble noble metal nanoparticles stabilized by small organic ligands that are synthesized by direct reduction, phase transfer, or redispersion methods have been investigated for a variety of catalytic reactions in water as described above. Typically, the direct reduction method allows the formation of water-soluble metal nanoparticles by the reduction of metal precursors directly in water. Another hydrophilic organic ligand or surfactant is often introduced to the reaction mixtures to further stabilize nanoparticles. The phase transfer method involves the formation of

nanoparticles in organic phase which is followed by the hydrophilic ligand-induced transfers of nanoparticles from organic phase to aqueous phase. The redispersion method is based on the reduction of water-insoluble metal precursors in mixed solvents. The subsequent solvent removal allows the dissolution of isolated hydrophilic metal nanoparticles in pure water.

These studies indicated that various hydrophilic capping ligands could be used for the stabilization of metal nanoparticles with potential applications in aqueous catalysis. Water-soluble Pd nanoparticles have been studied for a variety of reactions including the hydrogenation of unsaturated hydrocarbons, nitro compounds, and carbonyls, dehalogenation, hydrolysis, C-C coupling reactions, and C-H activations. Pt nanoparticles were active for mostly hydrogenation reactions such as alkene, arene, nitro, and carbonyl hydrogenations. Water-soluble Ru nanoparticles were found to have excellent reactivity towards alkene, arene, ammonia-borane, and carbonyl hydrogenations. In addition, Ru nanoparticles could be used for C-H activation and dye decomposition. Rh nanoparticles have been investigated for the hydrogenations of arenes, nitro compounds, carbonyls, and ammonia boranes in addition to the dehalogenation reaction. In comparison, the catalysis of water-soluble Au and Ag nanoparticles have been limited to nitro reductions, carbonyl hydrogenations, and dye decomposition. The catalysis application of Ir nanoparticles has only appeared for arene hydrogenation. The activity of metal nanoparticle catalysts were found to be highly dependent upon the type and structure of organic ligands that control the electronic properties of metal core and/or the accessibility of incoming substrates. Various water-soluble organic ligand-stabilized metal nanoparticle catalysts have also shown the abilities to catalyze regio-, chemo-, and stereoselective organic reactions, with the ligand often playing an important role in directing their activity and selectivity through the interactions with substrates.

Future studies should seek to enhance further understanding on critical structure-function relationships and technological applications of water-soluble organic molecular ligand-capped metal nanoparticle catalysts. This will require more systematic studies on the effect of the surface ligands with controlled structure, functionality, and packing density. Investigating the influence of well-defined organic ligands on metal nanoparticles resembling amino acid residues can provide understanding on the effects of steric, non-covalent, and chiral interactions in the near-surface environment (or near active site). Further advancements of this research using metal nanoparticle catalysts functionalized with well-defined small organic ligands with different hydrophobic or hydrophilic groups, therefore, can ultimately provide critical information regarding how nanocatalysts can tune catalytic selectivity precisely through specific substrate interactions. The future research should also continuously seek to develop different methods for the synthesis of nanoparticle catalysts that have a balance between catalytic activity and stability. It is also essential to mention that a critical issue in metal nanoparticle-catalyzed reactions is the mechanistic nature of these processes. For example, researchers have often diverged as to whether the nanoparticle catalysis arises from leached metals or nanoparticles themselves.[132] This question has been the subject of intense debate in the past decade and require well designed materials and well planned experiments to be free of controversy.

Besides their important roles in organic catalysis, water-soluble metal nanoparticles could also play critical roles in biocatalysis in addition to environmental applications such as waste decomposition and green catalysis. The continued investigations of small organic molecule-capped water-soluble metal nanoparticle catalysts will likely have a large impact on the broad field of research in science and technology. In specific, several studies focusing on the development of water-soluble metal nanoparticles for biocatalysis have appeared and the results

have been promising, yet much studies are left to be done in this field.[31-34] The catalytic property of metal nanoparticles optimized for organic reactions relevant to metabolisms, pro-drug activation, bio-labeling, etc. can be further investigated for clinical translation. By using readily adaptable organic ligand chemistry and metal core control, water-soluble ligand-stabilized metal nanoparticles can be tailored towards desired properties and functionalities. With the water solubility and design flexibility, new water-soluble metal nanoparticles with improved activity and selectivity can be prepared for aiming significant roles in biomedicine. The incorporation of metal nanoparticles with catalytic activity into biomolecules such as proteins and lipids might further expand their utilities in bioorthogonal catalytic reactions and allow for the development of new therapeutic strategies in living systems.[133-137] The bio-compatible catalytic nano-hybrids might allow highly efficient reactions inside multicellular organisms.

AUTHOR INFORMATION

Corresponding Author

* E-mail: ys.shon@csulb.edu. Phone: 562-985-4466. Fax: 562-985-8547.

Author Contributions

The manuscript was written through contributions of all authors. A-M.A. and Y.-S. S. wrote the original draft. Y.-S. S. supervised the project, provided resources and edited the draft. All authors have given approval to the final version of the manuscript.

Funding Sources

This work was funded by grants from the National Institute of General Medical Science of the National Institute of Health and the Division of Chemistry at National Science Foundation. The

funders had no role in the design of the study; in the collection, analyses, or interpretation of data; in the writing of the manuscript, or in the decision to publish the results.

ACKNOWLEDGMENT

We thank the National Institute of General Medical Science (GM089562), National Science Foundation (CHE-1954659), and CSULB for the financial supports.

ABBREVIATIONS

NPs, nanoparticles; AWLP6, anionic water-soluble leaning pillar[6]arene; TBAB, tetrabutylammonium bromide; DMAP, 4-dimethylaminopyridine; NHC, N-heterocyclic carbene; COD, 1,5-cyclooctadiene; COT, 1,3,5,7-cyclooctatetraene; SDS, sodium dodecylsufate; HP-CD, hydroxypropyl-α-cyclodextrin; HTAB, hydroxyl-functionalized tetraalkyl ammonium bromide; HTAC, hydroxyl-functionalized tetraalkyl ammonium chloride; Me-CD, methylated-α or β or γ-cyclodextrin; PHTAC, polyhydroxylated tetraalkyl ammonium chloride; OS-β-CD, oleic succinyl β-cyclodextrins; CTAB, cetyltrimethylammonium bromide; TOAB, tetraoctylammonium bromide; THF, tetrahydrofuran; DMF, *N,N*-dimethylformamide; TOF, turn-over frequency; HEA, *N*-alkyl-*N*-(2-hydroxyethyl)ammonium; CMC, critical micellar concentration; THEA16Cl, *N*-hexadecyl-*N*-tris-(2-hydroxyethyl) ammonium chloride; HPA16Cl, *N,N*-dimethyl-*N*-cetyl-*N*–(3-hydroxypropyl) ammonium chloride; GPI, gas projection impeller; rGO, reduced graphene oxide; NP, nitrophenol; NA, nitroaniline; GME, growing microelectrode; FGME, full-grown microelectrode; SPEG, thiolated polyethylene glycol; SPAA, thiolated poly(acrylic acid); MPA, 3-mercaptopropanoic acid; MHA, 6-mercaptohexanoic acid; MOA, 8-mercaptooctanoic acid; MUA, 11-mercaptoundecanoic acid; p-MBA, *para*-mercaptobenzoic

acid; TA, tannic acid; HEAnX, N,N-dimethyl-N-alkyl-N-(2-hydroxyethyl)ammonium halide; SG, glutathione; NMeEph12X, N-methylephedrium salts; .

REFERENCES

1) Nájera, C.; Beletskaya, I. P.; Yus, M. Metal-Catalyzed Regiodivergent Organic Reactions. *Chem. Soc. Rev.* **2019**, *48*, 4515-4618. DOI: 10.1039/c8cs00872h.

2) Cheng, W.-M.; Shang, R. Transition Metal-Catalyzed Organic Reactions under Visible Light: Recent Developments and Future Perspectives. *ACS Catal*. **2020**, *10(16)*, 9170-9196. DOI: 10.1021/acscatal.0c01979.

3) Shin, K.; Kim, H.; Chang, S. Transition-Metal-Catalyzed C-N Bond Forming Reactions Using Organic Azides as the Nitrogen Source: A Journey for the Mild and Versatile C-H Amination. *Acc. Chem. Res.* **2015**, *48(4)*, 1040-1052. DOI: 10.1021/acs.accounts.5b00020.

4) Trowbridge, A.; Walton, S. M.; Gaunt, M. J. New Strategies for the Transition-Metal Catalyzed Synthesis of Aliphatic Amines. *Chem. Rev.* **2020**, *120(5)*, 2613-2692. DOI: 10.1021/acs.chemrev.9b00462.

5) Kim, D.-S.; Park, W.-J.; Jun, C.-H. Metal-Organic Coorperative Catalysis in C-H and C-C Bond Activation. *Chem. Rev.* **2017**, *117(13)*, 8977-9015. DOI: 10.1021/acs.chemrev.6b00554.

6) Wang, D.; Astruc, D. The Golden Age of Transfer Hydrogenation. *Chem. Rev.* **2015**, *115*, 6621-6686. DOI; 10.1021/acs.chemrev.5b00203.

7) Yang, F.; Deng, D.; Pan, X.; Fu, Q.; Bao, X. Understanding Nano Effects in Catalysis. *Nat. Sci. Rev.* **2015**, *2*, 183-201. DOI: 10.1093/nsr/nwv024.

8) Rodrigues, T. S.; da Silva, A. G. M.; Camargo, P. H. C. Nanocatalysis by Noble Metal Nanoparticles: Controlled Synthesis for the Optimization and Understanding of Activities. *J. Mater. Chem. A* **2019**, *7*, 5857-5874. DOI: 10.1039/c9ta00074g.

9) Du, Y.; Sheng, H.; Astruc, D.; Zhu, M. Atomically Precise Nobel Metal Nanoclusters as Efficient Catalysts: A Bridge between Structure and Properties. *Chem. Rev.* **2020**, *120*, 526-622. DOI: 10.1021/acs.chemrev.8b00726.

10) Axet, M. R.; Philippot, K. Catalysis with Colloidal Ruthenium Nanoparticles. *Chem. Rev.* **2020**, *120*, 1085-1145. DOI: 10.1021/acs.chemrev.9b00434.

11) San, K. A.; Shon, Y.-S. Synthesis of Alkanethiolate-Capped Metal Nanoparticles Using Alkyl Thiosulfate Ligand Precursors: A Method to Generate Promising Reagents for Selective Catalysis. *Nanomaterials* **2018**, *8*, 346. DOI: 10.3390/nano8050346.

12) Gavia, D. J.; Shon, Y.-S. Catalytic Properties of Unsupported Palladium Nanoparticle Surfaces Capped with Small Organic Ligands. *ChemCatChem* **2015**, *7*, 892-900. DOI: 10.1002/cctc.201402865.

13) Sankar, M.; He, Q.; Engel, R. V.; Sainna, M. A.; Logsdail, A. J.; Roldan, A.; Willock, D. J.; Agarwal, N.; Kiely, C. J.; Hutchings, G. J. Role of the Support in Gold-Containing Nanoparticles as Heterogeneous Catalysts. *Chem. Rev.* **2020**, *120*, 3890-3938. DOI: 10.1021/acs.chemrev.9b00662.

14) Zhu, Q.-L.; Xu, Q. Immobilization of Ultrafine Metal Nanoparticles to High-Surface-Area Materials and Their Catalytic Applications. *Chem* **2016**, *1*, 220-245. DOI: 10.1016/j.chempr.2016.07.005.

15) Song, H. Metal Hybrid Nanoparticles for Catalytic Organic and Photochemical Transformations. *Acc. Chem. Res.* **2015**, *48*, 491-499. DOI: 10.1021/ar500411s.

16) Rossi, L. M.; Fiorio, J. L.; Garcia, M. A. S.; Ferraz, C. P. The Role and Fate of Capping Ligands in Colloidally Prepared Metal Nanoparticle Catalysts. *Dalton Trans.* **2018**, *47*, 5889-5915. DOI: 10.1039/c7dt04728b.

17) Campisi, S.; Schiavoni, M.; Chan-Thaw, C. E.; Villa, A. Untangling the Role of the Capping Agent in Nanocatalysis: Recent Advances and Perspectives. *Catalysts* **2016**, *6*, 185. DOI: 10.3390/catal6120185.

18) Niu, Z.; Li, Y. Removal and Utilization of Capping Agents in Nanocatalysis. *Chem. Mater.* **2014**, *26*, 72-83. DOI: 10.1021/cm4022479.

19) Schoenbaum, C. A.; Schwartz, D. K.; Medlin, J. W. Controlling the Surface Environment of Heterogeneous Catalysts Using Self-Assembled Monolayers. *Acc. Chem. Res.* **2014**, *47*, 1438-1445. DOI: 10.1021/ar500029y.

20) Vargas, K. M.; San, K. A.; Shon, Y.-S. Isolated Effects of Surface Ligand Density on the Catalytic Activity and Selectivity of Palladium Nanoparticles. *ACS Appl. Nano Mater.* **2019**, *2(11)*, 7188-7196. DOI: 10.1021/acsanm.9b01696.

21) Mahdaly, M. A.; Zhu, J. S.; Nguyen, V.; Shon, Y.-S. Colloidal Palladium Nanoparticles for Selective Hydrogenation of Styrene Derivatives with Reactive Functional Groups. *ACS Omega* **2019**, *4*, 20819-20828. DOI: 10.1021/acsomega.9b03335.

22) Chen. T.-A.; Shon, Y.-S. Alkanethiolate-Capped Palladium Nanoparticles for Regio- and Stereoselective Hydrogenation of Allenes. *Catalysts* **2018**, *8*, 428. DOI: 10.3390/catal8100428.

23) Chen, T.-A.; Shon, Y.-S. Alkanethioate-Capped Palladium Nanoparticle for Selective Catalytic Hydrogenation of Dienes and Trienes. *Catal. Sci. Technol.* **2017**, *7*, 4823-4829. DOI: 10.1039/C7CY01880K.

24) Maung, M. S.; Shon, Y.-S. Effects of Noncovalent Interactions on the Catalytic Activity of Unsupported Colloidal Palladium Nanoparticles Stabilized with Thiolate Ligands. *J. Phys. Chem. C* **2017**, *121*, 20882-20891. DOI: 10.1021/acsjpcc.7b07109.

25) Zhu, J. S.; Shon, Y.-S. Mechanistic Interpretation of Selective Catalytic Hydrogenation and Isomerization of Alkenes and Dienes by Ligand Deactivated Pd Nanoparticles. *Nanoscale* **2015**, *7*, 17786-17790. DOI: 10.1039/C5NR05090A.

26) Gavia, D. J.; Koeppen, J.; Sadeghmoghaddam, E.; Shon, Y.-S. Tandem Semi-hydrogenation/Isomerization of Propargyl Alcohols to Saturated Carbonyl Analogues by Dodecanethiolate-Capped Palladium Nanoparticle Catalysts. *RSC Adv.* **2013**, *3*, 13642-13645. DOI: 10.1039/c3ra42119h.

27) Narayan, N.; Meiyazhagan, A.; Vajtai, R. Metal Nanoparticles as Green Catalysts. *Materials* **2019**, *12*, 3602. DOI: 10.3390/ma12213602.

28) Denicourt-Nowicki, A.; Roucoux, A. From Hydroxycetylammonium Salts to Their Chiral Counterparts. A Library of Efficient Stabilizers of Rh(0) Nanoparticles for Catalytic Hydrogenation in Water. *Catal. Today* **2015**, *247*, 90-95. DOI: 10.1016/j.cattod.2014.05.031.

29) Yan, N.; Xiao, C.; Kou, Y. Transition Metal Nanoparticle Catalysts in Green Solvents. *Coord. Chem. Rev.* **2010**, *254*, 1179-1218. DOI: 10.1016/j.ccr.2010.02.015.

30) Chase, Z. A.; Fulton, J. L.; Camaioni, D. M.; Mei, D.; Balasubramanian, M.; Pham, V.-T.; Zhao, C.; Weber, R. S.; Wang, Y.; Lercher, J. A. State of Supported Pd during Catalysis in Water. *J. Phys. Chem. C* **2013**, *117*, 17603-17612. DOI: 10.1021/jp404772p.

31) Zhang, Y.; Li, S.; Liu, H.; Long, W.; Zhang, X.-D. Enzyme-Like Properties of Gold Clusters for Biomedical Application. *Front. Chem.* **2020**, *8*, 219. DOI: 10.3389/fchem.2020.00219.

32) Wang, Y.; Cai, R.; Chen, C. The Nano-Bio Interactions of Nanomedicines: Understanding the Biochemical Driving Forces and Redox Reactions. *Acc. Chem. Res.* **2019**, *52*, 1507-1518. DOI: 10.1021/acs.accounts.9b00126.

33) Soldevila-Barreda, J. J.; Metzler-Nolte, N. Intracellular Catalysis with Selected Metal Complexes and Metallic Nanoparticles: Advances toward the Development of Catalytic Metallodrugs. *Chem. Rev.* **2019**, *119*, 829-869. DOI: 10.1021/acs.chemrev.8b00493.

34) Hühn, J.; Carrillo-Carrion, C.; Soliman, M. G.; Pfeiffer, C.; Valdeperez, D.; Masood, A.; Chakraborty, I.; Zhu, L.; Gallego, M.; Yue, Z.; Carril, M.; Feliu, N.; Escudero, A.; Alkilany, A. M.; Pelaz, B.; del Pino, P.; Parak, W. J. Selected Standard Protocols for the Synthesis, Phase Transfer, and Characterization of Inorganic Colloidal Nanoparticles. *Chem. Mater.* **2017**, *29*, 399-461. DOI: 10.1021/acs.chemmater.6b04738.

35) Ishida, Y.; Suzuki, J.; Akita, I.; Yonezawa, T. Ultrarapid Cationization of Gold Nanoparticles vis a Single-Step Ligand Exchange Reaction. *Langmuir* **2018**, *34*, 10668-10672. DOI: 10.1021/acs.langmuir.8b02226.

36) Sakai, N.; Tatsuma, T. One-step Synthesis of Glutathione-Protected Metal (Au, Ag, Cu, Pd, and Pt) Cluster Powders. *J. Mater. Chem. A* **2013**, *1*, 5915-5922. DOI: 10.1039/c3ta00644a.

37) Zhang, H.; Yang, Y.; Dai, W.; Yang, D.; Lu, S.; Ji, Y. An Aqueous-Phase Catalytic Process for the Selective Hydrogenation of Acetylene with Monodisperse Water Soluble Palladium Nanoparticles as Catalyst. *Catal. Sci. Tech.* **2012**, *2*, 1319-1323. DOI:/10.1039/c2cy20179h.

38) Wang, B.; Ran, M.; Fang, G.; Wu, T.; Tian, Q.; Zheng, L.; Romero-Zerón, L.; Ni, Y. Palladium Nano-Catalyst Supported on Cationic Nanocellulose-Alginate Hydrogel for Effective Catalytic Reactions. *Cellulose* **2020**, *27*, 6995-7008. DOI:10.1007/s10570-020-03127-4.

39) Johnson, J. A.; Makis, J. J.; Marvin, K. A.; Rodenbusch, S. E.; Stevenson, K. J. Size-Dependent Hydrogenation of p-Nitrophenol with Pd Nanoparticles Synthesized with Poly(amido)amine Dendrimer Templates. *J. Phys. Chem. C* **2013**, *117*, 22644-22651. DOI:10.1021/jp4041474.

40) Deraedt, C.; Melaet, G.; Ralston, W. T.; Ye, R.; Somorjai, G. A. Platinum and Other Transition Metal Nanoclusters (Pd, Rh) Stabilized by PAMAM Dendrimers as Excellent Heterogeneous Catalysts: Application to the Methylcyclopentane (MCP) Hydrogenative Isomerization. *Nano Lett.* **2017**, *17*, 1853-1862. DOI:10.1021/acs.nanolett.6b05156.

41) Narayanan, R.; El-Sayed, M. A. Effect of Colloidal Catalysis on the Nanoparticle Size Distribution: Dendrimer-Pd vs PVP-Pd Nanoparticles Catalyzing the Suzuki Coupling Reaction. *J. Phys. Chem. B* **2004**, *108*, 8572-8580. DOI:10.1021/jp037169u.

42) Matsuo, A.; Hasegawa, S.; Takano, S.; Tsukuda, T. Electron-Rich Gold Clusters Stabilized by Poly(vinylpyridines) as Robust and Active Oxidation Catalysts. *Langmuir* **2020**, *36*, 7844-7849. DOI:10.1021/acs.langmuir.0c00812.

43) Gual, A.; Delgado, J. A.; Godard, C.; Castillón, S.; Curulla-Ferré, D.; Claver, C. Novel Polymer Stabilized Water Soluble Ru-Nanoparticles as Aqueous Colloidal Fischer-Tropsch Catalysis. *Top Catal*. **2013**, *56*, 1208-1219. DOI: 10.1007/s11244-013-0087-1.

44) de O. Santos, K.; Elias, W. C.; Signori, A. M.; Giacomelli, F. C.; Yang, H.; Domingos, J. B. *J. Phys. Chem. C* **2012**, *116*, 4594-4604. DOI:10.1021/jp2087169.

45) Saha, M.; Pal, A. K.; Nandi, S. Pd(0) NPs: A Novel and Reusable Catalyst for the Synthesis of Bis(heterocyclyl)methanes in Water. *RSC Adv.* **2012**, *2*, 6397-6400. DOI: 10.1039/c2ra20445b.

46) Nagata, T.; Obora, Y. N,N-Dimethylformamide-Protected Single Sized Metal Nanoparticles and Their Use as Catalysts for Organic Transformations. *ACS Omega* **2020**, *5*, 98-103. DOI: 10.1021/acsomega.9b03828.

47) Yamamoto, K.; Imaoka, T.; Tanabe, M.; Kambe, T. New Horizon of Nanoparticle and Cluster Catalysis with Dendrimer. *Chem. Rev*. **2020**, *120*, 1397-1437. DOI: 10.1021/acs.chemrev.9b00188.

48) Ye, R.; Zhukhovitskiy, A. V.; Deraedt, C. V.; Toste, F. D.; Somorjai, G. A. Supported Dendeimer-Encapsulated Metal Clusters: Toward Heterogenizing Homogeneous Catalysts. *Acc. Chem. Res.* **2017**, *50*, 1894-1901. DOI: 10/1021/acs.accounts.7b00232.

49) Myers, V. S.; Weir, M. G.; Carino, E. V.; Yancey, D. F.; Pande, S.; Crooks, R. M. Dendrimer-Encapsulated Nanoparticles: New Synthetic and Characterization Methods and Catalytic Applications. *Chem. Sci.* **2011**, *2*, 1632-1646. DOI: 10.1039/c1sc00256b.

50) Shifrina, Z. B.; Matveeva, V. G.; Bronstein, L. M. Role of Polymer Structures in Catalysis by Transition Metal and Metal Oxide Nanoparticle Composites. *Chem. Rev.* **2020**, *120*, 1350-1396. DOI: 10.1021/acs.chemrev.9b00137.

51) Wang, C.; Ciganda, R.; Salmon, L.; Gregurec, D.; Irigoyen, J.; Moya, S.; Ruiz, J.; Astruc, D. Highly Efficient Transition Metal Nanoparticle Catalysts in Aqueous Solution. *Angew. Chem. Int. Ed.* **2016**, *55*, 3091-3095. DOI: 10.1002/anie.201511305.

52) Scholten, J. D.; Leal, B. C.; Dupont, J. Transition Metal Nanoparticle Catalysis in Ionic Liquids. *ACS Catal.* **2012**, *2*, 184-200. DOI: 10.1021/cs200525e.

53) Abe, H.; Liu, J.; Ariga, K. Catalytic Nanoarchitectonics for Environmentally Compatible Energy Generation. *Mater. Today* **2016**, *19*, 12-18. DOI: 10.1016/j.mattod.2015.08.021.

54) Lohse, S. E.; Murphy, C. J. Applications of Colloidal Inorganic Nanoparticles: From Medicine to Energy. *J. Am. Chem. Soc.* **2012**, *134*, 15607-15620. DOI: 10.1021/ja307589n.

55) Denicourt-Nowicki, A.; Roucoux, A. From Hydroxycetylammonium Salts to Their Chiral Counterparts. A Library of Efficient Stabilizers of Rh(0) Nanoparticles for Catalytic Hydrogenation in Water. *Catal. Today* **2015**, *247*, 90-95. DOI:10.1016/j.cattod.2014.05.031.

56) Gual, A.; Godard, C.; Castillón, S.; Claver, C. Soluble Transition-Metal Nanoparticles-Catalysed Hydrogenation of Arenes. *Dalton Trans.* **2010**, *39*, 11499-11512. DOI:10.1039/c0dt00584c.

57) Denicourt-Nowicki, A.; Roucoux, A. Noble Metal Nanoparticles Stabilized by Cyclodextrins: A Pertinent Partnership for Catalytic Applications. *Curr. Org. Chem.* **2010**, *14*, 1266-1283.

58) Heiligtag, F. J.; Niederberger, M. The Fascinating World of Nanoparticle Research. *Mater. Today* **2013**, *16*, 262-271. DOI:10/1016/j.mattod.2013.07.004.

59) Turkevich, J.; Stevenson, P. C.; Hillier, J. A Study of the Nucleation and Growth Processes in the Synthesis of Colloidal Gold. *Discuss. Faraday Soc.* **1951**, *11*, 55-75. DOI: 10.1039/df9511100055.

60) Kimling, J.; Okenve, M. B.; Kotaidis, V.; Ballot, H.; Plech, A. Turkevich Method for Gold Nanoparticle Synthesis Revisited. *J. Phys. Chem. B* **2006**, *110*, 15700-15707. DOI: 10.1021/jp061667w.

61) Wuithschick, M.; Birnbaum, A.; Witte, S.; Sztucki, M.; Vainio, U.; Pinna, N.; Rademann, K.; Emmerling, F.; Kraehnert, R.; Polte, J. Turkevich in New Robes: Key Questions Answered for the Most Common Gold Nanoparticle Synthesis. *ACS Nano* **2015**, *9*, 7052-7071. DOI: 10.1021/acsnano.5b01579.

62) Piella, J.; Bastús, N. G.; Puntes, V. Size-Controlled Synthesis of Sub-10-nanometer Citrate-Stabilized Gold Nanoparticles and Related Optical Properties. *Chem. Mater.* **2016**, *28*, 1066-1075. DOI:10.1021/acs.chemmater.5b04406.

63) Bastús, N. G.; Merkoci, F.; Piella, J.; Puntes, V. Synthesis of Highly Monodisperse Citrate-Stabilized Silver Nanoparticles of up to 200 nm: Kinetic Control and Catalytic Properties. *Chem. Mater.* **2014**, *26*, 2836-2846. DOI:10.1021/cm500316k.

64) Li, G.; Zeng, C.; Jin, R. Chemoselective Hydrogenation of Nibrobenzaldehyde to Nitrobenzyl Alcohol with Unsupported Au Nanorod Catalysts in Water. *J. Phys. Chem. C* **2015**, *119*, 11143-11147. DOI:10.1021/jp511930n.

65) Chakraborty, S.; Ansar, S. M.; Stroud, J. G.; Kitchens, C. L. Comparison of Colloidal versus Supported Gold Nanoparticle Catalysis. *J. Phys. Chem. C* **2018**, *122*, 7749-7758. DOI:10.1021/acs.jpcc.8b00664.

66) Ansar, S. M.; Kitchens, C. L. Impact of Gold Nanoparticle Stabilizing Ligands on the Colloidal Catalytic Reduction of 4-Nitrophenol. *ACS Catal.* **2016**, *6*, 5553-5560. DOI:10.1021/acscatal.6b00635.

67) Ansar, S. M.; Fellows, B.; Mispireta, P.; Mefford, O. T.; Kitchens, C. L. pH Triggered Recovery and Reuse of Thiolated Poly(acrylic acid) Functionalized Gold Nanoparticles with Applications in Colloidal Catalysis. *Langmuir* **2017**, *33*, 7642-7648. DOI:10.1021/acs.langmuir.7b00870.

68) Bakr, E. A.; El-Attar, H. G.; Salem, M. A. Colloidal Ag@Pd Core-Shell Nanoparticles Showing Fast Catalytic Eradication of Dyes from Water and Excellent Antimicrobial Behavior. *Res. Chem. Intermed.* **2019**, *45*, 1509-1526. DOI:10.1007/s11164-018-3679-3.

69) Park, J.-W.; Shumaker-Parry, J. S. Strong Resistance of Citrate Anions on Metal Nanoparticles to Desorption under Thiol Functionalization. *ACS Nano* **2015**, *9*, 1665-1682. DOI:10.1021/nn506379m.

70) Kim, T. Y.; Park, Y. Green Synthesis and Catalytic Activity of Gold Nanoparticles/Graphene Oxide Nanocomposites Prepared by Tannic Acid. *J. Nanosci. Nanotechnol.* **2018**, *18*, 2536-2546. DOI:10.1166/jnn.2018.14389.

71) Wang, W.; Ciganda, R.; Wang, C.; Escobar, A.; Martinez-Villacorta, A. M.; Ramirez, M. A.; Hernández, R.; Moya, S. E.; Ruiz, J.; Hamon, J.-R.; Astruc, D. High Catalytic Activity of Rh

Nanoparticles Generated from Cobaltocene and $RhCl_3$ in Aqueous Solution. *Inorg. Chem. Front.* **2019**, *6*, 2704-2708. DOI:10.1039/c9qi00742c.

72) Monopoli, A.; Calò, V.; Ciminale, F.; Cotugno, P.; Angelici, C.; Cioffi, N.; Nacci, A. Glucose as a Clean and Renewable Reductant in the Pd-Nanoparticle-Catalyzed Reductive Homocoupling of Bromo- and Chloroarenes in Water. *J. Org. Chem.* **2010**, *75*, 3908-3911. DOI:10.1021/jo1005729.

73) Wang, X.; Wu, J.-R.; Liang, F.; Yang, Y.-W. In Situ Gold Nanoparticle Synthesis Mediated by a Water-Soluble Leaning Pillar[6]arene for Self-Assembly, Detection, and Catalysis. *Org. Lett.* **2019**, *21*, 5215-5218. DOI:10.1021/acs.orglett.9b01827.

74) Huang, T.; Meng, F.; Qi, L. Facile Synthesis and One-Dimensional Assembly of Cyclodextrin-Capped Gold Nanoparticles and Their Applications in Catalysis and Surface-Enhanced Raman Scattering. *J. Phys. Chem. C* **2009**, *113*, 13636-13642. DOI:10.1021/jp903405y.

75) Senra, J. D.; Malta, L. F. B.; da Costa, M. E. H. M.; Michel, R. C.; Aguiar, L. C. S.; Simas, A. B. C.; Antunes, O. A. C. Hydroxypropyl-a-Cyclodextrin-Capped Palladium Nanoparticles: Active Scaffolds for Efficient Carbon-Carbon Bond Forming Cross-Couplings in Water. *Adv. Synth. Catal.* **2009**, *351*, 2411-2422. DOI:10.1002/adsc.200900348.

76) Ranu, B. C.; Chattopadhyay, K. A New Route to the Synthesis of (E)- and (Z)-2-Alkene-4-ynoates and Nitriles from vic-Diiodo-(E)-alkenes Catalyzed by Pd(0) Nanoparticles in Water. *Org. Lett.* **2007**, *9*, 2409-2412. DOI:10.1021/ol0708121.

77) Saha, M.; Pal, A. K.; Nandi, S. Pd(0) NPs: A Novel and Reusable Catalyst for the Synthesis of Bis(heterocyclyl)methanes in Water. *RSC Adv.* **2012**, *2*, 6397-6400. DOI:10.1039/c2ra20445b.

78) Zhang, Z.; Zha, Z.; Gan, C.; Pan, C.; Zhou, Y.; Wang, Z.; Zhou, M.-M. Catalysis and Regioselectivity of the Aqueous Heck Reaction by Pd(0) Nanoparticles Under Ultrasonic Irradiation. *J. Org. Chem.* **2006**, *71*, 4339-4342. DOI:10.1021/jo060372b.

79) Schulz, J.; Roucoux, A.; Patin, H. Unprecedented Efficient Hydrogenation of Arenes in Biphasic Liquid-Liquid Catalysis by Re-Usable Aqueous Colloidal Suspensions of Rhodium. *Chem. Commun.* **1999**, 535-536.

80) Schulz, J.; Roucoux, A.; Patin, H. Stabilized Rhodium(0) Nanoparticles: A Reusable Hydrogenation Catalyst for Arene Derivatives in a Biphasic Water – Liquid System. *Chem. Eur. J.* **2000**, *6*, 618-624.

81) Schulz, J.; Levigne, S.; Roucoux, A.; Patin, H. Aqueous Rhodium Colloidal Suspension in Reduction of Arene Derivatives in Biphasic System: A Significant Physico-chemical Role of Surfactant Concentration on Catalytic Activity. *Adv. Synth. Catal.* **2002**, *344*, 266-269.

82) Nowicki, A.; Le Boulaire, V.; Roucoux, A. Nanoheterogeneous Catalytic Hydrogenation of Arenes: Evaluation of the Surfactant-Stabilized Aqueous Ruthenium(0) Colloidal Suspension. *Adv. Synth. Catal.* **2007**, *349*, 2326-2330. DOI:10.1002/adsc.200700208.

83) Hubert, C.; Denicourt-Nowicki, A.; Roucoux, A.; Landy, D.; Leger, B.; Crowyn, G.; Monflier, E. Catalytically Active Nanoparticles Stabilized by Host-Guest Inclusion Complexes in Water. *Chem. Commun.* **2009**, 1228-1230. DOI:10.1039/b818786j.

84) Hubert, C.; Bilé, E. G.; Denicourt-Nowicki, A.; Roucoux, A. Tandem Dehalogenation-Hydrogenation Reaction of Halogenoarenes as Model Substrates of Endocrine Disruptors in Water: Rhodium Nanoparticles in Suspension vs. on Silica Support. *Appl. Catal. A: General* **2011**, *394*, 215-219. DOI:10.1016/j.apcata.2011.01.004.

85) Roucoux, A.; Schulz, J.; Patin, H. Arene Hydrogenation with a Stabilised Aqueous Rhodium(0) Suspension: A Major Effect of the Surfactant Counter-Anion. *Adv. Synth. Catal.* **2003**, *345*, 222-229.

86) Bilé, E. G.; Sassine, R.; Denicourt-Nowicki, A.; Launay, F.; Roucoux, A. New Ammonium Surfactant-Stabilized Rhodium(0) Colloidal Suspensions: Influence of Novel Counter-Anions on Physico-Chemical and Catalytic Properties. *Dalton Trans.* **2011**, *40*, 6524-6531. DOI:10.1039/c0dt01763a.

87) Nowicki, A.; Zhang, Y.; Léger, B.; Rolland, J.-P.; Bricout, H.; Monflier, E.; Roucoux, A. Supramolecular Shuttle and Protective Agent: A Multiple Role of Methylated Cyclodextrins in the Chemoselective Hydrogenation of Benzene Derivatives with Ruthenium Nanoparticles. *Chem. Commun.* **2006**, 296-298. DOI:10.1039/b512838b.

88) Denicourt-Nowicki, A.; Ponchel, A.; Monflier, E.; Roucoux, A. Methylated Cyclodextrins: An Efficient Protective Agent in Water for Zerovalent Ruthenium Nanopartices and a Supromolecular Shuttle in Alkene and Arene Hydrogenation Reactions. *Dalton Trans.* **2007**, 5714-5719. DOI:10.1039/b713989f.

89) Bilé, E. G.; Denicourt-Nowicki, A.; Sassine, R.; Beaunier, P.; Launary, F.; Roucoux, A. N-Methylephedrium Salts as Chiral Surfactants for Asymmetric Hydrogenation in Neat Water

with Rhodium(0) Nanocatalysts. *ChemSusChem* **2010**, *3*, 1276-1279. DOI: 10.1002/cssc.201000206.

90) Hubert, C.; Denicourt-Nowicki, A.; Guégan, J.-P.; Roucoux, Polyhydroxylated Ammonium Chloride Salt: A New Efficient Surfactant for Nanoparticles Stabilisation in Aqueous Media. Characterization and Application in Catalysis. *Dalton Trans.* **2009**, 7356-7358. DOI:10.1039/b911094a.

91) Cocq, A.; Léger, B.; Noël, S.; Bricout, H.; Djedaïni-Pilard, F.; Tilloy, S.; Monflier, E. Anionic Amphiphilic Cyclodextrins Bearing Oleic Grafts for the Stabilization of Ruthenium Nanoparticles Efficient in Aqueous Catalytic Hydrogenation. *ChemCatChem* **2020**, *12*, 1013-1018. DOI:10.1002/cctc.201901837.

92) Mévellec, V.; Roucoux, A.; Ramirez, E.; Philippot, K.; Chaudret, B. Surfactant-Stabilized Aqueous Iridium(0) Colloidal Suspension: An Efficient Reusable Catalyst for Hydrogenation of Arenes in Biphasic Media. *Adv. Synth. Catal.* **2004**, *346*, 72-76. DOI:10.1002/adsc.200303157.

93) Léger, B.; Nowicki, A.; Roucoux, A.; Rolland, J.-P. Competitive Hydrogenation/Dehalogenation of Halogenoarenes with Surfactant-Stabilized Aqueous Suspensions of Rhodium and Palladium Colloids: A Major Effect of the Metal Nature. *J. Mole. Catal. A: Chemical* **2007**, *266*, 221-225. DOI:10/1016/j.molcata.2006.11.004.

94) Denicourt-Nowicki, A.; Romagné, M.-L.; Roucoux, A. N-(2-Hydroxyethyl)ammonium Derivatives as Protective Agents for Pd(0) Nanocolloids and Catalytic Investigation in Suzuki Reactions in Aqueous Media. *Catal. Commun.* **2008**, *10*, 68-70. DOI:10.1016/j.catcom.2008.07.023.

95) Sullivan, J. A.; Flanagan, K. A.; Hain, H. Selective H – D Exchange Catalysed by Aqueous Phase and Immobilised Pd Nanoparticles. *Catal. Today* **2008**, *139*, 154-160. DOI:10.1016/j.cattod.2008.03.031.

96) Rambabu, D.; Pradeep, C. P.; Dhir, A. New Self-Assembled Material Based on Ru Nanoparticles and 4-Sulfocalix[4]arene as an Efficient and Recyclable Catalyst for Reduction of Brilliant Yellow Azo Dye in Water: A New Model Catalytic Reaction. *J. Nanopart. Res.* **2016**, *18*, 381. DOI:10.1007/s11051-016-3693-6.

97) Li, J.; Nasaruddin, R. R.; Feng, Y.; Yang, J.; Yan, N.; Xie, J. Tuning the Accessibility and Activity of $Au_{25}(SR)_{18}$ Nanocluster Catalysts through Ligand Engineering. *Chem. Eur. J.* **2016**, *22*, 14816-14820. DOI:10.1002/chem.201603247.

98) Pradhan, N.; Pal, A.; Pal, T. Silver Nanoparticle Catalyzed Reduction of Aromatic Nitro Compounds. *Coll. Surf. A* **2002**, *196*, 247-257.

99) Grzeschik, R.; Schäfer, D.; Holtum, T.; Küpper, S.; Hoffmann, A.; Schlücker, S. On the Overlooked Critical Role of the pH Value on the Kinetics of the 4-Nitrophenol NaBH4-Reduction Catalyzed by Noble-Metal Nanoparticles (Pt, Pd, and Au). *J. Phys. Chem. C* **2020**, *124*, 2939-2944. DOI:10.1021/acs.jpcc.9b07114.

100) Martinez-Prieto, L. M; Baquero, E. A.; Pieters, G.; Flores, J. C.; de Jesús, E.; Nayral, C.; Delpech, F.; van Leeuwen, P. W. N. M.; Lippens, G.; Chaudret, B. Monitoring of Nanoparticle Reactivity in Solution: Interaction of L-Lysine and Ru Nanoparticles Probed by Chemical Shift Perturbation Parallels Regioselective H/D Exchange. *Chem. Commun.* **2017**, *53*, 5850-5853. DOI:10.1039/c7cc02445b.

101) Tay, B. Y.; Wang, C.; Phua, P. H.; Stubbs, L. P.; Huynh, H. V. Selective Hydrogenation of Levulinic Acid to γ-Valerolactone Using In Situ Generated Ruthenium Nanoparticles Derived from Ru-NHC Complexes. *Dalton Trans.* **2016**, *45*, 3558-3563. DOI:10.1039/c5dt03366g.

102) Mévellec, V.; Mattioda, C.; Schulz, J.; Rolland, J.-P.; Roucoux, A. Enantioselective Hydrogenation of Ethyl Pyruvate in Biphasic Liquid-Liquid Media by Reusable Surfactant-Stabilized Aqueous Suspensions of Platinum Nanoparticles. *J. Catal.* **2004**, *225*, 1-6. DOI: 10.1016/j.jcat.2004.03.017.

103) Durap, F.; Zahmakiran, M.; Özkar, S. Water Soluble Laurate-Stabilized Ruthenium(0) Nanoclusters Catalyst for Hydrogen Generation from the Hydrolysis of Ammonia-Borane: High Activity and Long Lifetime. *Int. J. Hydrog. Energy* **2009**, *34*, 7223-7230. DOI:10.1016/j.ijhydene.2009.06.074.

104) Durap, F.; Zahmakiran, M.; Özkar, S. Water Soluble Laurate-Stabilized Rhodium(0) Nanoclusters Catalyst with Unprecedented Catalytic Lifetime in the Hydrolytic Dehydrogenation of Ammonia-Borane. *Appl. Catal. A: General* **2009**, *369*, 53-59. DOI:10.1016/j.apcata.2009.08.031.

105) Xu, S.; Yang, Q. Well-Dispersed Water-Soluble Pd Nanocrystals: Facile Reducing Synthesis and Application in Catalyzing Organic Reactions in Aqueous Media. *J. Phys. Chem. C* **2008**, *112*, 13419-13425. DOI:10.1021/jp800539x.

106) Thiery, E.; Bras, J. L.; Muzart, J. Palladium Nanoparticles-Catalyzed Regio- and Chemoselective Hydrogenolysis of Benzylic Epoxides in Water. *Green Chem.* **2007**, *9*, 326-327. DOI:10.1039/b616486b.

107) Zhou, C.; Wang, J.; Li, L.; Wang, R.; Hong, M. A Palladium Chelating Complex of Ionic Water-Soluble Nitrogen-Containing Ligand: The Efficient Precatalyst for Suzuki-Miyaura Reaction in Water. *Green Chem.* **2011**, *13*, 2100-2106. DOI:10.1039/c1gc15060j.

108) Saha, D.; Chattopadhyay, K.; Ranu, B. C. Aerobic Ligand-Free Suzuki Coupling Catalyzed by In Situ-Generated Palladium Nanoparticles in Water. *Tetrahedron Lett.* **2009**, *50*, 1003-1006. DOI:10.1016/j.tetlet.2008.12.063.

109) Gavia, D. J.; Maung, M. S.; Shon, Y.-S. Water-Soluble Pd Nanoparticles Synthesized from ω-Carboxyl-*S*-alkanethiosulfate Ligand Precursors as Unimolecular Micelle Catalysts. *ACS Appl. Mater. Interfaces* **2013**, *5*, 12432-12440. DOI: 10.1021/am4035043.

110) Maung, M. S.; Dinh, T.; Salazar, C.; Shon, Y.-S. Unsupported Colloidal Palladium Nanoparticles for Biphasic Hydrogenation and Isomerization of Hydrophobic Allylic Alcohols in Water. *Colloids Surf. A* **2017**, 513, 367-372. DOI: 10.1016/j.colsurfa.2016.10.067.

111) Chen, V.; Pan, H.; Jacobs, R.; Derakhshan, S.; Shon, Y.-S. Influence of Graphene Oxide Supports on Solution-Phase Catalysis of Thiolate-Protected Palladium Nanoparticles in Water. *New J. Chem.* **2017**, *41*, 177-183. DOI: 10.1039/C6NJ02898E.

112) Caporali, M.; Guerriero, A.; Ienco, A.; Caporali, S.; Peruzzini, M.; Gonsalvi, L. Water-Soluble, 1,3,5-Trizaz-7-phosphaadamantane-Stabilized Palladium Nanoparticles and Their Application in Biphasic Catalytic Hydrogenations at Room Temperature. *ChemCatChem* **2013**, *5*, 2517-2526. DOI:10.1002/cctc.201300079.

113) Guerrero, M.; Roucoux, A.; Denicourt-Nowicki, A.; Bricout, H.; Monflier, E.; Collière, V.; Fajerwerg, K.; Philippot, K. *Catal. Today* **2012**, *183*, 34-41. DOI:10.1016/j.cattod.2011.09.012.

114) Alvarez, J.; Liu, J.; Román, E.; Kaifer, A. E. Water-Soluble Platinum and Palladium Nanoparticles Modified with Thiolated β-Cyclodextrin. *Chem. Commun.* **2000**, 1151-1152. DOI:10.1039/b002423f.

115) Mhadgut, S. C.; Palaniappan, K.; Thimmaiah, M.; Hackney, S. A.; Török, B.; Liu, J. A Metal Nanoparticle-Based Supramolecular Approach for Aqueous Biphasic Reactions. *Chem. Commun.* **2005**, 3207-3209. DOI:10.1039/b502181b.

116) Xue, C.; Palaniappan, K.; Arumugam, G.; Hackney, S. A.; Liu, J.; Liu, H. Sonogashira Reactions Catalyzed by Water-Soluble, b-Cyclodextrin-capped Palladium Nanoparticles. *Catal. Lett.* **2007**, *116*, 94-101. DOI:10.1007/s10562-007-9108-7.

117) Gao, G.-Q.; Lin, L.; Fan, C.-M.; Zhu, Q.; Wang, R.-X.; Xu, A.-W. Highly Dispersed Platinum Nanoparticles Generated Viologen Micelles with High Catalytic Activity and Stability. *J. Mater. Chem. A* **2013**, *1*, 12206-12212. DOI:10.1039/c3ta12485a.

118) Li, G.; Jiang, D.; Kumar, S.; Chen, Y.; Jin, R. Size Dependence of Atomically Precise Gold Nanoclusters Chemoselective Hydrogenation and Active Site Structure. *ACS Catal.* **2014**, *4*, 2463-2469. DOI:10.1021/cs500533h.

119) Busacca, C. A.; Fandrick, D. R.; Song, J. J.; Senanayake, C. H. The Growing Impact of Catalysis in the Pharmaceutical Industry. *Adv. Syn. Catal.* **2011**, *353*, 1825-1864. DOI:10.1002/adsc.201100488.

120) Callis, N. M.; Thiery, E.; Bras, J. L.; Muzart, J. Palladium Nanoparticles-Catalyzed Chemoselective Hydrogenations, a Recyclable System in Water. *Tetrahedron Lett.* **2007**, *48*, 8128-8131. DOI:10.1016/j.tetlet.2007.09.121.

121) Sarikoç, S. *Fuels of the Diesel-Gasoline Engines and Their Properties.* In *Diesel and Gasoline Engines*: Viskup, R. Ed.; IntechOpen Limited, London, 2020; pp 31-46. DOI:10.5772/intechopen.89044.

122) Pelisson, C.-H.; Hubert, C.; Denicourt-Nowicki, A.; Roucoux, A. From Hydroxyalkylammonium Salts to Protected-Rh(0) Nanoparticles for Catalysis in Water: Comparative Studies of the Polar Heads. *Top Catal.* **2013**, *56*, 1220-1227. DOI:10.1007/s11244-013-0088-0.

123) Strachan, J.; Barnett, C.; Masters, A. F.; Maschmeyer, T. 4-Nitrophenol Reduction: Probing the Putative Mechanism of the Model Reaction. *ACS Catal.* **2020**, *10*, 5516-5521. DOI:10.1021/acscatal.0c00725.

124) Kovacic, P.; Somanathan, R. Nitroaromatic Compounds: Environmental Toxicity, Carcinogenicity, Mutagenicity, Therapy and Mechanism. *J. Appl. Toxicol.* **2014**, *34*, 810-824. DOI:10.1002/jat.2980.

125) Serna, P.; Corma, A. Transforming Nano Metal Nonselective Particulates into Chemoselective Catalysts for Hydrogenation of Substituted Nitrobenzenes. *ACS Catal.* **2015**, *5*, 7114-7121. DOI:10.1021/acscatal.5b01846.

126) Biffis, A.; Centomo, P.; Del Zotto, A.; Zecca, M. Pd Metal Catalysts for Cross-Couplings and Related Reactions in the 21st Century: A Critical Review. *Chem. Rev*. **2018**, *118*, 2249-2295. DOI:10.1021/acs.chemrev.7b00443.

127) Hong, K.; Sajjadi, M.; Suh, J. M.; Zhang, K.; Nasrollahzadeh, M.; Jang, H. W.; Varma, R. S.; Shokouhimehr, M. Palladium Nanoparticles on Assorted Nanostructured Supports: Applications for Suzuki, Heck, and Sonogashira Cross-Coupling Reactions. *ACS Appl. Nano Mater.* **2020**, *3*, 2070-2103. DOI:10.1021/acsanm.9b02017.

128) Yasukawa, T.; Miyamura, H.; Kobayashi, S. Chiral Rhodium Nanoparticle-Catalyzed Asymmetric Arylation Reactions. *Acc. Chem. Res.* **2020**, *53*, 2950-2963. DOI:10.1021/acs.accounts.0c00587.

129) Deraedt, C.; Astruc, D. "Homeopathin" Palladium Nanoparticle Catalysis of Cross Carbon-Carbon Coupling Reactions. *Acc. Chem. Res.* **2014**, *47*, 494-503. DOI:10.1021/ar400168s.

130) Sable, V.; Maindan, K.; Kapdi, A. R.; Shejwalkar, P. S.; Hara, K. Active Palladium Colloids via Palladacycle Degradation as Efficient Catalysts for Oxidative Homocoupling and Cross-Coupling of Aryl Boronic Acids. *ACS Omega* **2017**, *2*, 204-217. DOI:10.1021/acsomega.6b00326.

131) Eyimegwu, P. N.; Lartey, J. A.; Kim, J.-H. Gold-Nanoparticle-Embedded Poly(N-isopropylacrylamide) Microparticles for Selective Quasi-Homogeneous Catalytic Homocoupling Reactions. *ACS Appl. Nano Mater.* **2019**, *2*, 6057-6066. DOI:10.1021/acsanm.9b01594.

132) Sun, B.; Ning, L.; Zeng, H. C. Confirmation of Suzuki-Miyaura Cross-Coupling Reaction Mechanism through Synthetic Architecture of Nanocatalysts. *J. Am. Chem. Soc.* **2020**, *142*, 13823-13832. DOI:10.1021/jacs.0c04804.

133) Duss, M.; Vallooran, J. J.; Manni, L. S.; Kieliger, N.; Handschin, S.; Mezzenga, R.; Jessen, H. J.; Landau, E. M. Lipidic Mesophase-Embedded Palladium Nanoparticles: Synthesis

and Tunable Catalysts in Suzuki-Miyaura Cross-Coupling Reactions. *Langmuir* **2019**, *35*, 120-127. DOI:10.1021/acs.langmuir.8b02905.

134) Vargas, K. M.; Shon, Y.-S. Hybrid Lipid-Nanoparticle Complexes for Biomedical Applications. *J. Mater. Chem. B*, **2019**, *7*, 695-708. DOI: 10.1039/C8TB03084G.

135) Wang, G.; Castiglione, K. Light-Driven Biocatalysis in Liposomes and Polymersomes. Where Are We Now? *Catalysts* **2019**, *9*, 12. DOI:10.3390/catal9010012.

136) Hauer, B. Embracing Nature's Catalysts: A Viewpoint on the Future of Biocatalysis. *ACS Catal.* **2020**, *10*, 8418-8427. DOI:10.1021/acscatal.0c01708.

137) Devaraj. N. K. The Future of Bioorthogonal Chemistry. *ACS Cent. Sci.* **2018**, *4*, 952-959. DOI:10.1021/acscentsci.8b00251.

Table of Contents Only